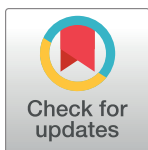


RESEARCH ARTICLE

Impact of secondary TCR engagement on the heterogeneity of pathogen-specific CD8⁺ T cell response during acute and chronic toxoplasmosis

Lindsey A. Shallberg¹, Anthony T. Phan¹, David A. Christian¹, Joseph A. Perry¹, Breanne E. Haskins¹, Daniel P. Beiting¹, Tajie H. Harris², Anita A. Koshy³, Christopher A. Hunter^{1*}



1 Department of Pathobiology, School of Veterinary Medicine, University of Pennsylvania, Philadelphia, Pennsylvania, United States of America, **2** Center for Brain Immunology and Glia, Department of Neuroscience, University of Virginia, Charlottesville, Virginia, United States of America, **3** Department of Neurology, Department of Immunobiology, and BIO5 Institute, University of Arizona, Tucson, Arizona, United States of America

* chunter@vet.upenn.edu

OPEN ACCESS

Citation: Shallberg LA, Phan AT, Christian DA, Perry JA, Haskins BE, Beiting DP, et al. (2022) Impact of secondary TCR engagement on the heterogeneity of pathogen-specific CD8⁺ T cell response during acute and chronic toxoplasmosis. PLoS Pathog 18(6): e1010296. <https://doi.org/10.1371/journal.ppat.1010296>

Editor: Eric Y. Denkers, University of New Mexico, UNITED STATES

Received: January 24, 2022

Accepted: May 6, 2022

Published: June 21, 2022

Peer Review History: PLOS recognizes the benefits of transparency in the peer review process; therefore, we enable the publication of all of the content of peer review and author responses alongside final, published articles. The editorial history of this article is available here: <https://doi.org/10.1371/journal.ppat.1010296>

Copyright: © 2022 Shallberg et al. This is an open access article distributed under the terms of the [Creative Commons Attribution License](#), which permits unrestricted use, distribution, and reproduction in any medium, provided the original author and source are credited.

Data Availability Statement: All RNAseq files are available from the GEO database (accession number GSE188495.).

Abstract

Initial TCR engagement (priming) of naive CD8⁺ T cells results in T cell expansion, and these early events influence the generation of diverse effector and memory populations. During infection, activated T cells can re-encounter cognate antigen, but how these events influence local effector responses or formation of memory populations is unclear. To address this issue, OT-I T cells which express the Nur77-GFP reporter of TCR activation were paired with the parasite *Toxoplasma gondii* that expresses OVA to assess how secondary encounter with antigen influences CD8⁺ T cell responses. During acute infection, TCR stimulation in affected tissues correlated with parasite burden and was associated with markers of effector cells while Nur77-GFP⁻ OT-I showed signs of effector memory potential. However, both Nur77-GFP⁻ and Nur77-GFP⁺ OT-I from acutely infected mice formed similar memory populations when transferred into naive mice. During the chronic stage of infection in the CNS, TCR activation was associated with large scale transcriptional changes and the acquisition of an effector T cell phenotype as well as the generation of a population of CD103⁺ CD69⁺ Trm like cells. While inhibition of parasite replication resulted in reduced effector responses it did not alter the Trm population. These data sets highlight that recent TCR activation contributes to the phenotypic heterogeneity of the CD8⁺ T cell response but suggest that this process has a limited impact on memory populations at acute and chronic stages of infection.

Author summary

Following priming, the ability of effector CD8⁺ T cells to recognize class I restricted microbial antigens is important to control many acute and chronic infections. However the role that recent T cell receptor stimulation plays in the formation of ongoing T cell

Funding: This study was funded by the National Institute of Allergy and Infectious Diseases (5R01AI157247; 5T32AI00753223, R01NS112516; CAH, AAK, THH, <https://www.nih.gov/>). The funders had no role in study design, data collection and analysis, decision to publish, or preparation of the manuscript.

Competing interests: The authors have declared that no competing interests exist.

responses is unclear. Here, we utilize a genetic reporter of TCR stimulation, high parameter flow cytometry, and imaging to characterize TCR-driven phenotypes of pathogen specific T cell responses to the parasite *Toxoplasma gondii* during acute and chronic infection in the periphery and central nervous system. These data sets highlight the contribution of recent TCR activation on the phenotypic heterogeneity of the CD8⁺ T cell response but suggest that T cell memory formation and maintenance is independent of recent TCR activation.

Introduction

CD8⁺ T cells play an important role in immunity to intracellular infections and multiple subsets including T effector, T memory, and T resident memory (Trm) cells have been associated with different anatomical locations and distinct functions [1–3]. During infection, dendritic cells in secondary lymphoid organs present microbially derived peptides via MHC Class I, activating T Cell Receptor (TCR) signaling of naive CD8⁺ T cells. This signal 1, along with co-stimulation (signal 2) and cytokines (signal 3) results in priming of naive CD8⁺ T cells and induces a proliferative burst. Consequently, an individual CD8⁺ T cell can produce 1,000 to 10,000 daughter cells within a week of stimulation, which in turn give rise to diverse effector and memory populations [4–10]. After priming, CD8⁺ T cells leave the secondary lymphoid organs and migrate to the periphery, where they can mediate TCR-dependent effector functions that include cytolysis of infected cells and secretion of cytokines (IFN- γ and TNF- α) required for resistance to infection. While early responses are dominated by the production of T effector populations it is clear that even during the early stage of infection that memory precursor populations are present [11,12]. As pathogen burden is controlled there is a contraction phase where the majority of effector CD8⁺ T cells undergo apoptosis, but a heterogeneous population of long-lived memory T cells remain in the circulation and reside in tissues [6,13,14]. During many chronic infections, a pool of effector and memory CD8⁺ T cells will persist that contribute to the long-term control of the pathogen [15–18]. Multiple studies have documented heterogeneity in the phenotype, function, longevity, and fate of these pathogen specific CD8⁺ T cells [8,12,19], but it is unclear whether re-encounter with cognate antigen at local sites of infection contributes to the observed diversity.

In current models, antigen experienced T cells are less dependent on signal 2 and 3, and stimulation through the TCR is considered the critical signal that induces local effector activities [20,21]. However, previously activated T cells can respond to signals 2 and 3 to mediate effector functions that include the production of cytokines such as IFN- γ [22–24]. The ability to assess T cell function and activation status at sites of infection and inflammation has depended on changes in the expression of surface proteins such as CD69, CD44 and LFA-1, the use of genetically encoded reporters of cytokine production or the ability to secrete cytokines on re-stimulation, and even intravital imaging of their behavior [25–27]. These approaches have been complimented by protein and transcriptional profiling that have highlighted phenotypic and functional heterogeneity of CD8⁺ T cells associated with different pathogens [1,28,29]. Nevertheless, certain combinations of surface molecules, such as chemokine receptors as well as activating or inhibitory receptors, have helped define different T cell subsets. For example, in certain viral and bacterial infections, the use of graded expression of the chemokine receptor CX3CR1 along with KLRG1 has been used to distinguish effector and memory CD8⁺ T cell populations [8,9]. Likewise, even during acute toxoplasmosis, the co-expression of cell surface receptors KLRG1 and CXCR3 distinguishes CD8⁺ T cell subsets that

have memory potential or are terminally differentiated, with continued presence of infection driving the KLRG1⁺CXCR3⁻ terminally differentiated population [12,30].

As a consequence of T cell activation, changes in the levels of surface markers such as LFA-1, CD44, and CD69 have been useful to identify antigen experienced T cell populations, but it has been a challenge to distinguish those T cell populations that have undergone recent TCR mediated activation [31]. Thus, while TCR signals promote a marked increase in CD69, this transmembrane C type lectin associated with tissue retention is also upregulated by inflammatory signals, its downregulation is varied and following clearance of antigen CD69 is constitutively expressed on Trm populations [32–35]. Genetically encoded reporters of calcium flux have been useful for imaging of TCR signals *in vivo* [25], however these calcium fluxes are rapid and transient and this method does not permit long term tracking or isolation of antigen stimulated cells. Nur77 is an orphan nuclear hormone receptor that is upregulated quickly following stimulation of the TCR [36–39] and transgenic mice that express Nur77-GFP have been used to identify T cells that have experienced recent TCR engagement during priming and the effector phase of T cell responses [36,37,40].

T. gondii is a ubiquitous obligate intracellular parasite that naturally infects many intermediate hosts, including humans and mice [41]. Resistance to this intracellular parasite is dependent on cell mediated immunity and as a natural host for this pathogen, the mouse has provided a tractable model that helped establish the role of IFN- γ and CD8⁺ T cells in resistance to intracellular infection [12,16,42–44]. In mice, early infection is characterized by high levels of replication of the tachyzoite stage of the parasite and vascular dissemination to multiple tissues [45–47]. This phase of infection generates a robust T cell response that restricts parasite growth, but the ability of *T. gondii* to form latent tissue cysts in neurons allows infection to persist in the CNS [44,48]. Depending on the combination of mouse and parasite strains the chronic phase of infection can be asymptomatic or lead to an ongoing encephalitis characterized by the presence of parasite specific T cells that provide robust local protection but which never fully resolves [49]. In the latter setting, there is good evidence that antigen is processed and presented within the CNS [50–52] and long-term control of *T. gondii* is mediated by CD4⁺ and CD8⁺ T cell production of IFN- γ which activates a variety of anti-microbial mechanisms [53–55]. Likewise in humans, chronic toxoplasmosis is considered to be largely asymptomatic but in patients with acquired defects in T cell responses, the reactivation of the tissue cysts can lead to the development of toxoplasmic encephalitis (TE) [41,56]. Analysis of the CD8⁺ T cell responses in murine models of acute and chronic toxoplasmosis has highlighted mechanisms that generate and sustain CD8⁺ T cell responses in the periphery [30,57–59] as well as the presence of a sub-population of Trm-like cell populations in the CNS [12,34,57] that are mirrored in other infections [13,60].

The ability to modify *T. gondii* to express model antigens such as ovalbumin (OVA), combined with TCR transgenics has provided an important tool to understand T cell responses to this infection [51,52,61–63]. This approach allowed the study of early events that lead to parasite specific T cell responses, how these operate in the CNS, and the cells that present antigen in the brain [12,50–52,64,65]. Here, OT-I CD8⁺ T cells specific for the OVA peptide SIINFEKL which express Nur77-GFP were combined with *T. gondii*-OVA, which constitutively express OVA in the tachyzoite and bradyzoite life stages, to identify cells that had recently engaged their TCR and assess how this impacted function. Although TCR activity has been linked to memory formation [66], an adoptive transfer model indicated that during the acute phase recent TCR stimulation did not influence the ability to form long lived memory T cells. During the chronic stage of infection, tachyzoite replication in the CNS was associated with TCR activation, large scale transcriptional changes, and the acquisition of an effector T cell phenotype as well as the generation of a local population of Trm like cells. However, while inhibition of

parasite replication resulted in reduced effector responses it did not alter the Trm population. These data sets highlight the contribution of recent TCR activation on the phenotypic heterogeneity of the CD8⁺ T cell response but suggest that T cell memory formation and maintenance is independent of recent TCR activation.

Results

*Nur77-GFP reporter detects recent *T. gondii*-mediated TCR activation*

To track TCR activation in a defined population of CD8⁺ T cells, transgenic mice were generated that express the OT-I TCR specific for the H2-Kb restricted SIINFKL peptide and the Nur77-GFP reporter (Nur77-GFP OT-I). As expected, naive Nur77-GFP OT-I stimulated with αCD3 *in vitro* induced expression of GFP within 45 minutes that peaked by 2 hours (Fig 1A). Removal of αCD3 following 48 hours of stimulation resulted in downregulation of GFP expression within 24–36 hours with basal levels by 72 hours (Fig 1B). This stimulation was accompanied by expression of CD69 which persisted after T cells were rested and had lost GFP expression (Fig 1C). When rested OT-I were restimulated with αCD3 there was rapid re-expression of Nur77-GFP (Fig 1C). The use of peptides with differing affinity for the OT-I TCR revealed a hierarchy wherein a low affinity peptide (EIINFEKL) did not induce reporter expression, moderate affinity peptides (SIIVFEKL and SIIQFEKL) induced intermediate levels of GFP, and the highest levels were associated with SIINFEKL (S1A Fig). To test whether Nur77-GFP OT-I encounter with endogenously processed OVA from an infected cell (as opposed to peptide pulsed cells or αCD3) would activate the reporter, bone marrow derived macrophages were infected *in vitro* with a non-replicating strain of *T. gondii* (CPS or CPS-OVA) and co-cultured with naive Nur77-GFP OT-I. With CPS-infected cells there was no induction of GFP and a modest impact on CD69, but co-culture with CPS-OVA infected cells resulted in high levels of GFP and co-expression of CD69 (Fig 1D). To determine if TCR-independent inflammatory signals during infection influence T cell expression of Nur77-GFP, 50,000 αCD3 and αCD28 pre-activated and rested Nur77-GFP OT-I T cells were transferred into mice infected for 10 days with the PRU strain of *T. gondii* or PRU expressing OVA (*T. gondii*-OVA). Although transfer of these T cells into mice infected with *T. gondii* that did not express OVA resulted in a modest increase of CD69, GFP expression was only observed when OT-I were transferred into *T. gondii*-OVA infected mice (Fig 1E). Thus, in the absence of cognate antigen the inflammatory environment is not sufficient to induce reporter expression. These *in vitro* and *in vivo* data sets validate that the expression of Nur77-GFP provides a sensitive and specific indicator of the recent interaction of OT-I CD8⁺ T cells with *T. gondii*-derived SIINFEKL.

*Infection induced kinetics and phenotype of *T. gondii* specific CD8 T cells*

Previous studies have shown infection with *T. gondii*-OVA results in the rapid clonal expansion of OT-I that is dependent on the presence of OVA, and that these OT-I can contribute to control of *T. gondii* [29,51,64]. To assess the frequency with which these primed T cells re-encounter antigen, 5,000 congenically distinct (CD45.1) naive Nur77-GFP OT-I were transferred into wild type CD45.2 recipients that were then infected intraperitoneally (i.p.) with 10,000 *T. gondii*-OVA parasites that expresses tdTomato. This is a low dose of infection that results in efficient priming and expansion of OT-I early in infection [51,65]. To focus on TCR mediated events after initial priming, mice were analyzed between 10 and 60 days post-infection (dpi). The number of live cells in the spleen that were positive for tdTomato revealed high parasite burden at 10 dpi with a marked decline by days 14 and 20 (Fig 2A). Starting at day 10 post-infection the OT-I in the spleen were all high for LFA-1, a marker of antigen experienced

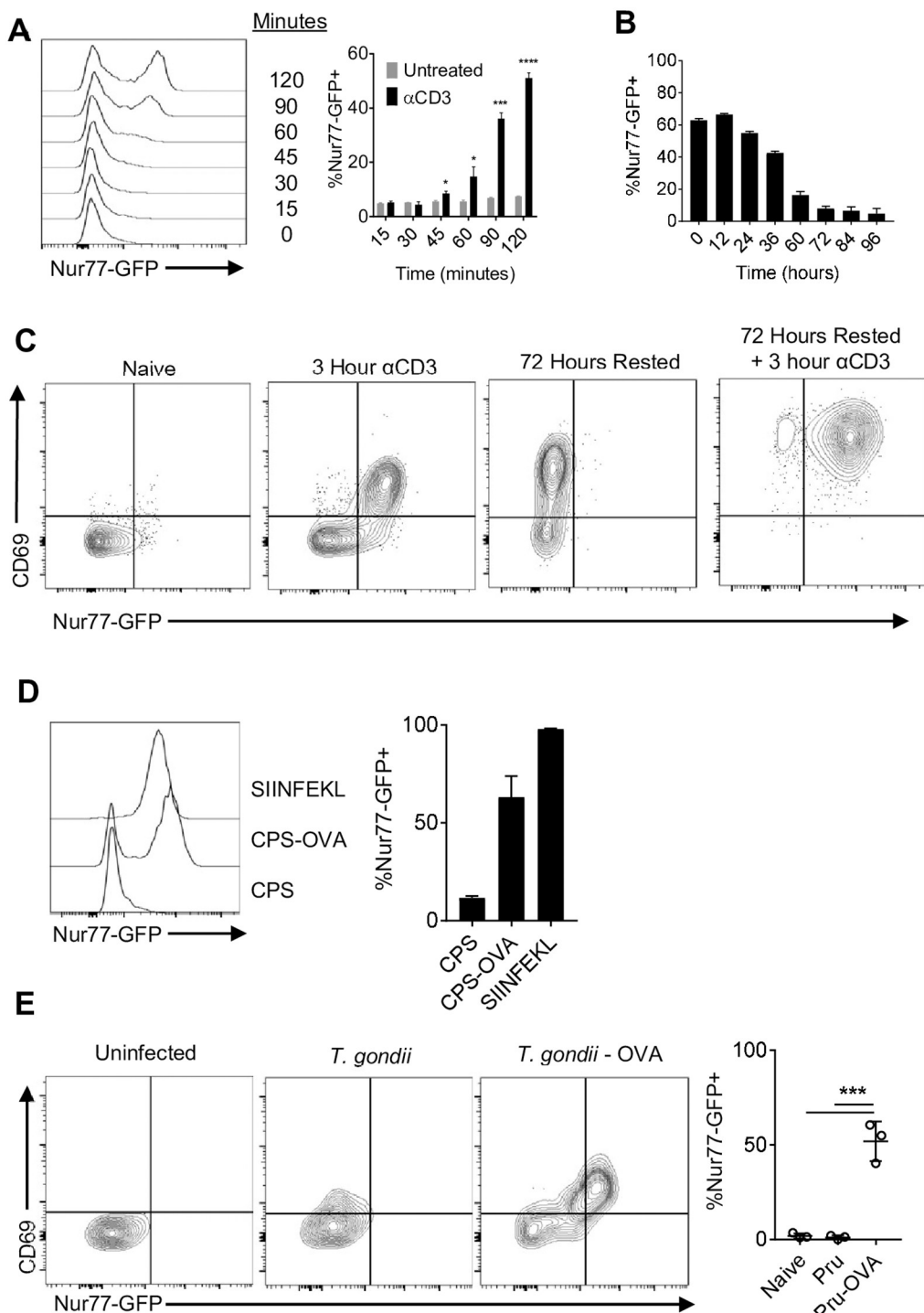


Fig 1. Nur77-GFP OT-I respond to *T. gondii* antigen. (A-B) Naive OT-I stimulated *in vitro* with plate bound α CD3 and α CD28 for up to 48 hours (A), then removed from stimulation (B) (N = 3 technical replicates per treatment per timepoint). (C) Rested OT-I restimulated with α CD3 (Representative of 3 technical replicates per treatment per timepoint). (D) BMDM infected with CPS or CPS-OVA and co-cultured with naive OT-I for 24 hours (N = 3 technical replicates per treatment per timepoint). (E) 50,000 OT-I pre-activated with α CD3 and α CD28 were transferred i.v. into mice infected with *T. gondii* or *T. gondii*-OVA at 10 dpi, and OT-I from the spleen were analyzed for Nur77-GFP expression at 10 days post transfer (N = 3 mice per group). P values based on Students T-test with Bonferroni-Dunn correction for multiple comparisons *p<0.05, ***p<0.001, ****p<0.0001; error bars indicate SD.

<https://doi.org/10.1371/journal.ppat.1010296.g001>

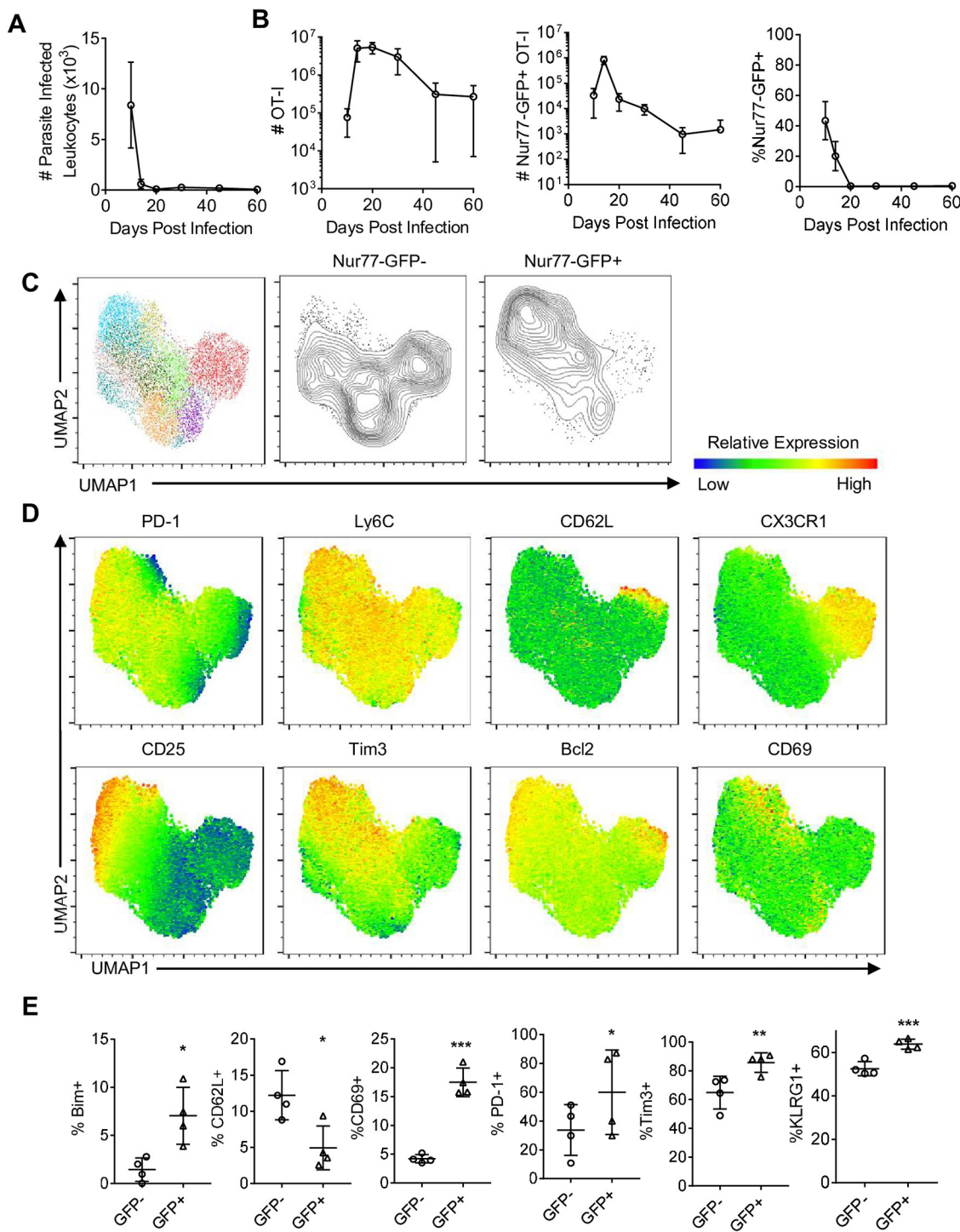


Fig 2. Infection induced kinetics and phenotype of splenic *T. gondii* specific CD8⁺ T cells. (A-B) OT-I were transferred i.v. into naive mice and infected with *T. gondii*-OVA. Mice were sacrificed between 10 and 60 dpi and spleens were analyzed (N = 3–5 mice per time point). (A) Number of parasite infected leukocytes per spleen as measured by flow cytometry. (B) Number of OT-I (left), number of Nur77-GFP⁺ OT-I (center), and frequency of Nur77-GFP⁺ OT-I of total OT-I (right) in the spleen. (C-E) High dimensional flow cytometry with UMAP and Phenograph clustering was performed on splenic OT-I at 10 dpi (N = 4 mice). (C) UMAP segregation of clusters of all OT-I (left), Nur77-GFP⁺ OT-I (center), and Nur77-GFP⁺ OT-I (right). (D) Heatmap of marker expression from UMAP. (E) Frequency of marker positive OT-I within Nur77-GFP⁻ or Nur77-GFP⁺ OT-I fraction. P values based on Paired T-test *p<0.05, **p<0.01, ***p<0.001; error bars indicate SD.

<https://doi.org/10.1371/journal.ppat.1010296.g002>

T cells, their numbers peaked at 14 dpi and the contraction was apparent by 20 dpi (Fig 2B). Mirroring pathogen burden, at 10 dpi GFP⁺ OT-I in the spleen were readily detected with peak numbers at day 14 (Fig 2B). As parasite burden declined, there was a marked reduction in the numbers and frequency of GFP⁺ OT-I (Fig 2B).

To determine whether recent TCR stimulation is associated with a distinct phenotype, OT-I were analyzed by high-parameter flow cytometry using markers associated with effector and memory precursor populations (see [Materials and Methods](#) for full panel) at 10 dpi. Phenograph clustering indicated that these T cells that had not seen recent TCR appeared as five major clusters, one characterized by the expression of CX3CR1 and CD62L and another associated with reduced expression of activation markers such as CD25 (IL-2R α) and PD-1 (Fig 2C). In contrast, a majority of GFP⁺ OT-I were defined by expression of CD25, PD-1, Bim, and Bcl-2, but were low for CX3CR1 and CD62L (Fig 2D and 2E). Additionally, GFP⁺ OT-I were more likely to be positive for KLRG1 (an inhibitory receptor expressed by effector T cells) (Fig 2E). Thus, at the peak of the T cell response in the periphery, recent TCR activation is most closely associated with those T cells that express markers of an effector population.

Secondary TCR activation does not impact on ability to form memory

Previous studies have highlighted the impact of TCR activation on the formation of memory populations and the observation that the majority of GFP⁻ OT-I were KLRG1⁺ CX3CR1⁺, whereas the GFP⁺ OT-I were largely KLRG1⁺ CX3CR1⁻ (Figs 3A and S2A) suggested that these populations may have different memory potential. To determine if recent antigen stimulation affected the ability to generate memory cell populations, GFP⁻ and GFP⁺ OT-I were sorted from the spleen of day 10 *T. gondii*-OVA infected mice and transferred into naive mice (Fig 3B and 3C). This process did not lead to infection, based on the absence of tdTomato⁺ cells and lack of GFP expression in the transferred OT-I (S2B and S2C Fig). Nevertheless, 14 days post transfer, OT-I were present in the spleens of these mice but there was no difference in the number of OT-I recovered from the two experimental groups (Fig 3D). In addition, despite differences in the expression of CX3CR1 prior to transfer, the memory cell populations in the mice were all characterized by high expression of CX3CR1 and KLRG1 (Figs 3E and S2D), as well as other effector and memory markers such as CXCR3 (S2E Fig). These data suggest the population of TCR stimulated cells at day 10 retain the ability to give rise to an effector memory population characterized by co-expression of KLRG1 and CX3CR1.

Influence of TCR stimulation on T cell responses in the CNS

In B6 mice infected with type II strains of *T. gondii* (including PRU), the parasite enters the CNS as a tachyzoite and there is sustained tachyzoite replication and foci of parasite replication associated with areas of inflammation are readily apparent [45,67]. As T cell responses lead to local parasite control, the ability to form tissue cysts (that contain bradyzoites) within neurons allows persistent infection, although periodic reactivation of cysts leads to the resumption of the lytic cycle [68,69]. Indeed, parasites were detected in the CNS at 10 dpi and the number of tachyzoite infected leukocytes declined between days 20 and 30, although total parasite burden remained high through 40 dpi (Fig 4A). OT-I were recruited to the brain between 10 and 14 dpi (Fig 4B) when ~40% of these cells expressed GFP which decreased to ~10–20% of OT-I at 2 months post infection (Fig 4B). The high percentage of GFP⁺ cells in the CNS at 10 dpi is at a time point when T cells enter the CNS but infected endothelial cells in the blood vessels are present [45]. To distinguish the OT-I T cells in the vascular compartment from those that had

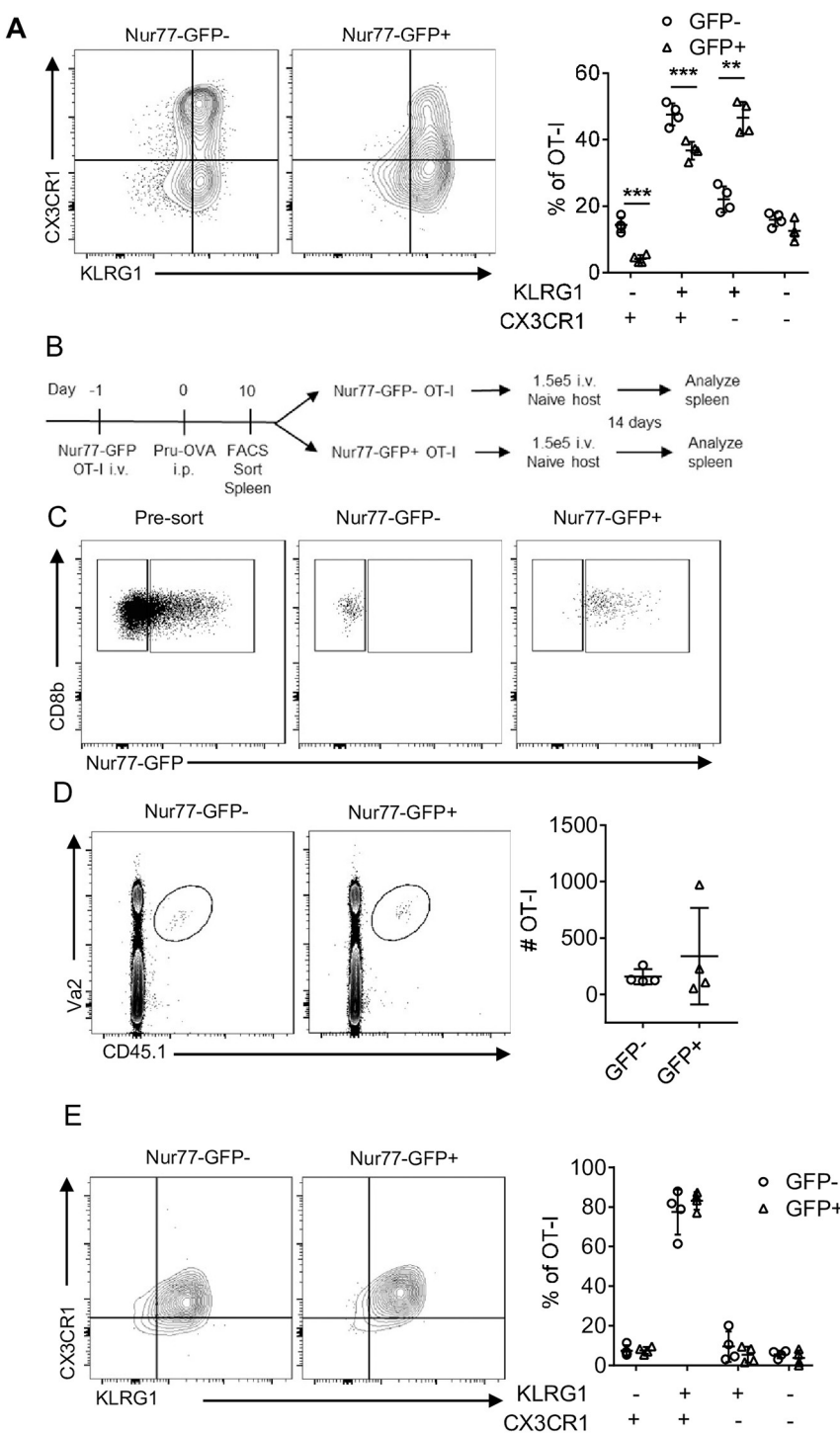


Fig 3. CD8⁺ T cell memory potential retained in Nur77-GFP⁺ OT-I. (A) OT-I from spleen of *T. gondii*-OVA 10 dpi (N = 4 mice). (B-C) OT-I from spleen of *T. gondii*-OVA 10 dpi were sorted by Nur77-GFP expression and transferred into naive mice. Mice were sacrificed 14 days post transfer (N = 4 mice). (D) Identification of OT-I from mice receiving either Nur77-GFP⁺ or Nur77-GFP⁻ OT-I. (E-F) Characterization of OT-I from recipient mice. P values based on Students T-test with Bonferroni-Dunn correction for multiple comparisons **p<0.01, ***p<0.001; error bars indicate SD.

<https://doi.org/10.1371/journal.ppat.1010296.g003>

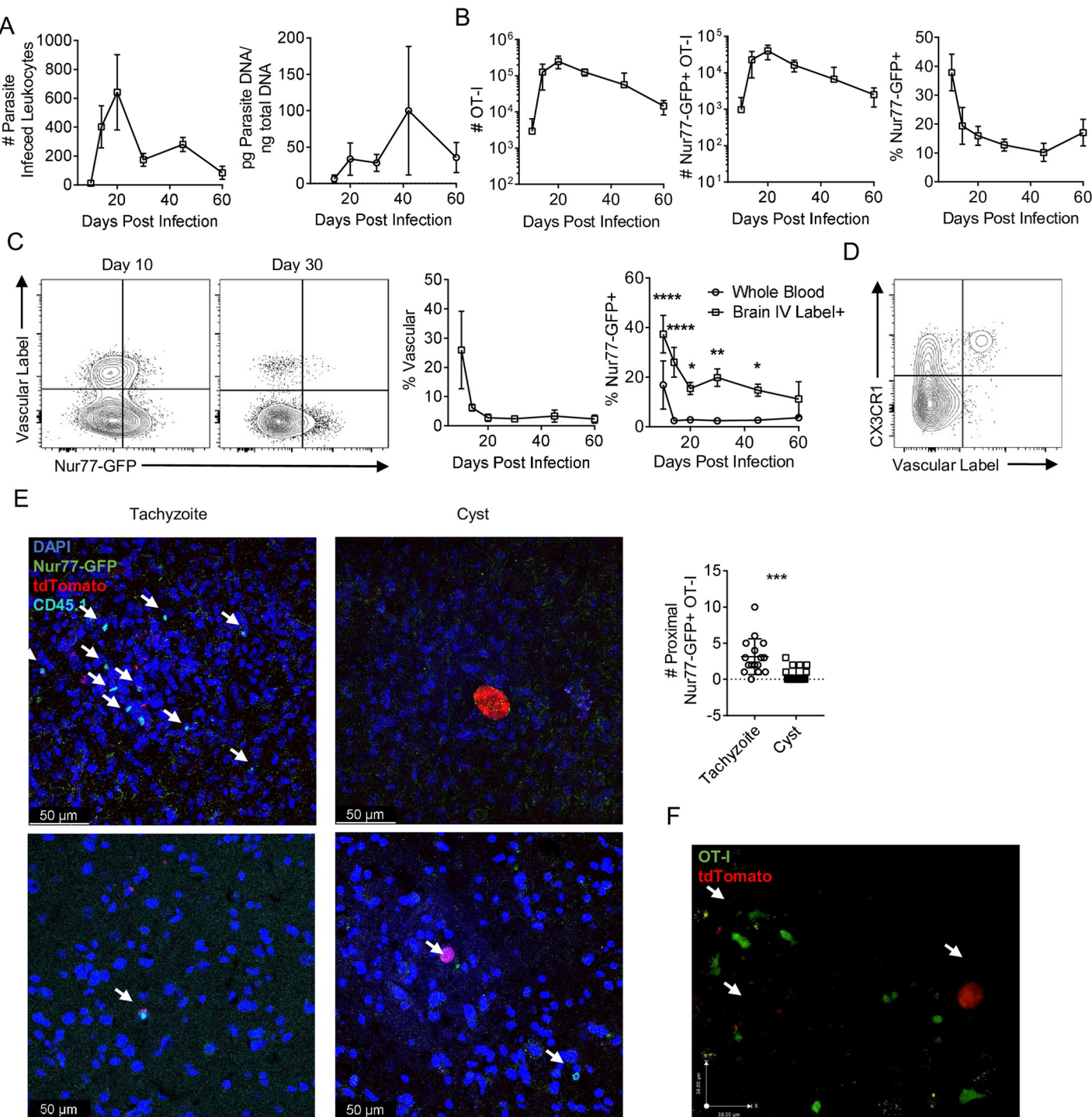


Fig 4. Infection induced kinetics of CNS *T. gondii* specific CD8⁺ T cells. (A-B) Kinetics of infection and OT-I in the brain following infection with *T. gondii*-OVA ($N = 3\text{--}4$ mice per time point). (A) Number of parasite infected leukocytes per brain as measured by flow cytometry (left) and total brain parasite burden as measured by parasite PCR (right). (B) Number of OT-I (left), number of Nur77-GFP⁺ OT-I (center), and frequency of Nur77-GFP⁺ OT-I of total OT-I (right) in the brain. (C-D) Mice were given i.v. dose of fluorophore conjugated αCD45 prior to sacrifice to label vascular cells. OT-I from whole blood were compared to OT-I from the vascular labeled fraction of the brain. The frequency of vascular⁺ OT-I in the brain was measured (left) and the frequency of Nur77-GFP⁺ OT-I out of all OT-I in the whole blood versus the vascular⁺ OT-I in the brain was compared (right). ($N = 3\text{--}4$ mice per timepoint). P values based on Two-Way ANOVA * $p < 0.05$ ** $p < 0.01$ **** $p < 0.0001$; error bars indicate SD. (D) Nur77-GFP⁺ OT-I from the CNS of *T. gondii*-OVA infected mice at 10 dpi. (E) Brain sections from 28 dpi were stained for CD45.1 (cyan) to identify OT-I, anti-GFP (green) to identify recently TCR stimulated OT-I, DAPI (blue) to identify nuclei, and were infected with *T. gondii*-OVA expressing tdTomato (red). Number of Nur77-GFP⁺ OT-I surrounding parasites were counted. Arrows indicate Nur77-GFP⁺ OT-I (representative of images from

N = 4 mice). (F) *Ex vivo* imaging of constitutive GFP expressing OT-I (green) in brain explants of *T. gondii*-OVA (red) infected mice. Arrows indicate *T. gondii* infection. P values based on Students T-test ***p<0.001; error bars indicate SD.

<https://doi.org/10.1371/journal.ppat.1010296.g004>

crossed into the parenchyma of the brain, fluorophore conjugated α CD45 was administered i.v. 3 minutes prior to sacrifice to label vascular resident cells and these populations were compared with those in whole blood. At 10 dpi in the whole blood ~20% of OT-I were GFP⁺, with a rapid decline in GFP expression by 14 dpi (Fig 4C) which correlated with the clearance of parasites from circulation. In the CNS at 10 dpi, ~30% of OT-I were vascular and ~40% of these vascular OT-I expressed Nur77-GFP (Fig 4C). By 20 dpi, this frequency of brain vascular OT-I had dropped to <5% (Fig 4C) and expression of GFP in these OT-I cells was <20% (Fig 4C). At 10 dpi when OT-I are entering the CNS, vascular associated Nur77-GFP⁺ OT-I were positive for CX3CR1 (Fig 4D), a chemokine receptor involved in T cell trafficking.

To determine if there was any differential association in the brain of GFP⁺ OT-I with areas of parasite replication, IHC was used to visualize fluorescent parasites, CD45.1⁺ OT-I T cells, and staining for GFP at day 28. OT-I were widely dispersed throughout the CNS and the majority were Nur77-GFP⁻, and these cells were not typically associated with areas of parasite replication. In contrast, Nur77-GFP⁺ OT-I were readily observed in association with areas of tachyzoite replication (Fig 4E). In addition, it was noted that a small number of GFP⁺ cells were detected in the vicinity of the parasite cysts, which also express OVA (Fig 4E). Similar results could be detected using live imaging of infected mice, but in which the OT-I did not express the Nur77-GFP reporter, but rather expressed GFP under the control of the CD4 promoter, as previously described [51]. In this setting, congregation of OT-I around areas of tachyzoite replication, with OT-I that are actively infected by parasite were readily identified (S1 Movie). It was also notable that in this movie OT-I T cells that were non-motile and had a rounded appearance (two behaviors associated with TCR engagement) could be visualized in proximity to a cyst. Together, these data sets highlight that early in infection that OT-I encounter antigen outside the CNS, but as the infection transitions to the CNS there are enhanced levels of TCR activation that occur at the interface between the brain and the vascular system, and in the chronic phase TCR activity is most closely associated with sites of parasite replication versus latent cysts.

Impact of TCR engagement on CD8⁺ T cells during toxoplasmic encephalitis

To assess the impact of recent TCR stimulation on the CD8⁺ T cell population in the CNS, GFP⁻ and GFP⁺ populations of OT-I T cells from the brains of mice infected for 14 days were analyzed by RNA sequencing. Principal component analysis revealed that GFP⁻ and GFP⁺ OT-I formed distinct clusters (S3A Fig) and over 2,000 genes were differentially regulated between these populations (adjusted P-value <0.05, logFC >0.3, Fig 5A). In GFP⁻ OT-I, transcripts for multiple transcription factors associated with memory precursor formation and longevity were upregulated (Fig 5B). The transcriptional profile of GFP⁺ OT-I was characteristic of effector T cells and associated with an enrichment of the surface receptors *Cx3cr1* and *Il2ra*, and transcriptional factors (such as *Zeb2* and *Irf8*), as well as those involved in negative regulation of T cell responses (*Egr2* and *Egr3*, Fig 5B). Moreover, an unbiased GSEA analysis revealed the top enriched gene sets of the GFP⁺ OT-I were associated with immune cell activation and anti-pathogen responses (S1 Table). As expected, the GFP⁺ OT-I were also enriched for gene sets associated with effector functions such as cytotoxicity and IFN- γ production (Fig 5C). This analysis also revealed enrichment of gene sets involved in the negative regulation of

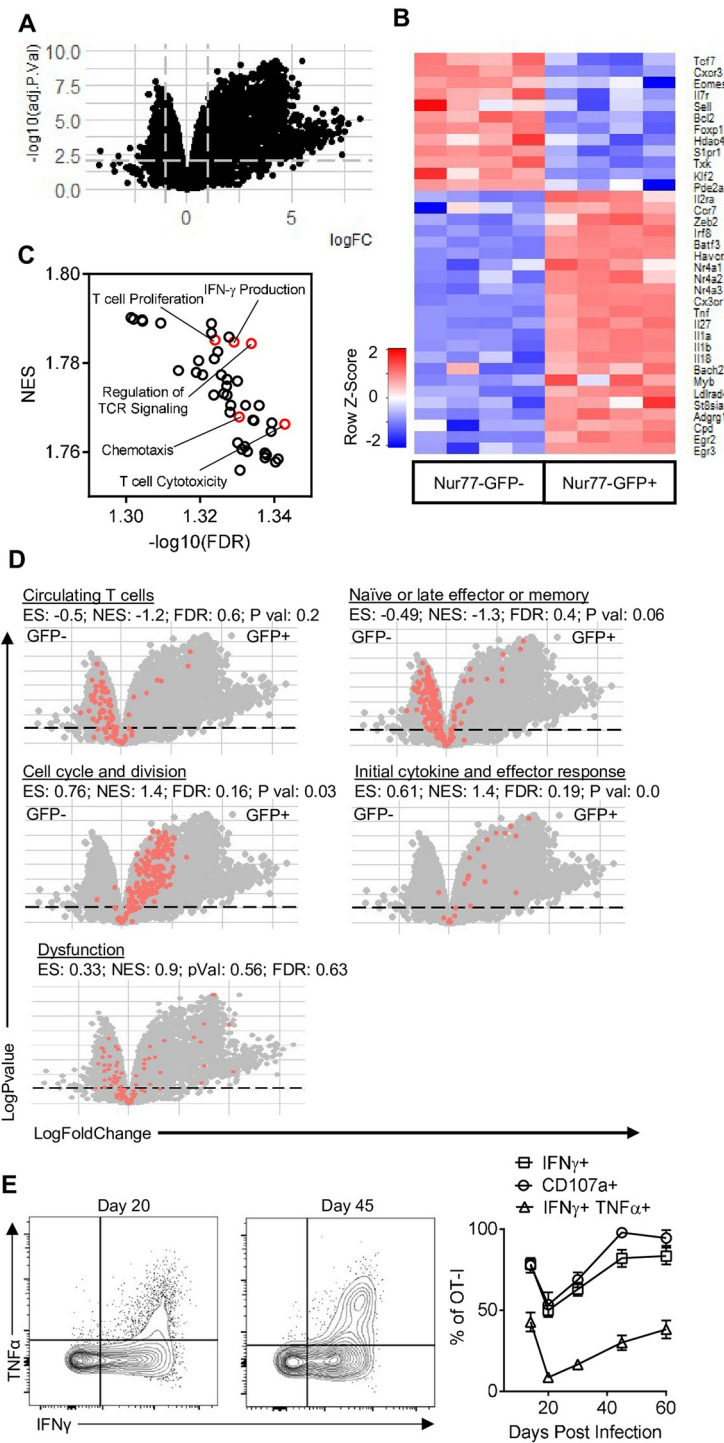


Fig 5. Transcriptional profiling of Nur77-GFP OT-I from CNS. (A-D) Nur77-GFP⁻ and Nur77-GFP⁺ OT-I from the brains of mice infected with *T. gondii*-OVA 14 dpi were transcriptionally profiled using RNA-sequencing (N = 4 pools of 2 mice per pool). (A) Volcano plot of all transcripts. Lines indicate logFC > 0.03 and adjusted P-value > 0.05. (B) Heatmap of differentially expressed genes involved in CD8+ T cell activation, differentiation, memory formation, and effector function. (C) Top GSEA enriched pathways in Nur77-GFP⁺ OT-I compared to Nur77-GFP⁻ OT-I. (D) Gene sets involved in CD8+ T cell activation and differentiation (red dots). (E) OT-I from brains of *T. gondii*-OVA infected mice were restimulated with SIINFEKL peptide and cytokine and degranulation was assessed by flow cytometry (N = 3–5 mice per group per timepoint).

<https://doi.org/10.1371/journal.ppat.1010296.g005>

TCR mediated signaling (Fig 5C), indicating that an inhibitory feedback loop for TCR signaling was already engaged in those cells.

To determine the differentiation status of GFP⁻ vs GFP⁺ OT-I, direct comparison of these subsets with gene signatures derived from LCMV specific CD8⁺ T cells at different points of infection [1] was performed. This analysis highlighted that GFP⁻ OT-I had greater abundance of transcripts connected with circulating T cells, as well as signatures associated with late effector CD8⁺ T cells (Fig 5D). Similar to the GSEA analysis (Fig 5C), the GFP⁺ OT-I were enriched for early effector molecules and anti-pathogen responses, as well as genes involved in cell division (Fig 5D). Although these T cells express multiple inhibitory receptors such as PD-1, there was no enrichment of a complete set of dysfunction related genes in either the GFP⁻ or GFP⁺ OT-I at this time point (Fig 5D). Previous studies have described the presence of a Trm-like population in the CNS during TE that produce the cytokines IFN-γ and TNF-α [34], and the Trm associated transcripts (*Cpd* and *Adgrg1*) were enriched in GFP⁺ OT-I, whereas transcripts that are decreased in Trm (*S1pr1* and *Klf2*) had lower abundance in GFP⁺ OT-I (Fig 5C). Furthermore, when the basal (i.e., not restimulated) ability of OT-I T cells in the brain to produce cytokines was assessed, GFP⁺ OT-I were 5 times more likely to be producing IFN-γ than GFP⁻ OT-I (S3B Fig). For the OT-I T cells isolated from the brain between 14 and 60 dpi and stimulated with SIINFEKL peptide, the majority of these produced IFN-γ or TNF-α, and degranulated (based on CD107a expression, Fig 5E). These data indicate that local TCR activation, rather than bystander activation, is the main stimulus required for effector function during TE and that at these time points there is no overt signature of T cell exhaustion.

Based in part on the transcriptional profiling, high parameter flow cytometry for a panel of markers of activation, memory, exhaustion, and transcription factors was employed to compare the Nur77-GFP OT-I T cell response in the spleen and brain at 2 and 6 weeks post infection. At 14 dpi OT-I phenotypes were distinct between the spleen and brain, with KLRG1 and CX3CR1 co-expression higher in the spleen than brain (Fig 6A). Unsupervised clustering of the brain OT-I at this time point identified 11 unique populations (Fig 6B). There were 7 clusters that were independent of recent TCR activation, and 4 clusters associated with Nur77-GFP expression (Fig 6B). Clusters that contained the GFP⁺ OT-I were also enriched for expression of KLRG1, CX3CR1, Tim3, CD25, Ki67 and Bcl-2 (Fig 6C and 6D). One of the most notable differences between Nur77-GFP⁻ and Nur77-GFP⁺ OT-I in the brain is illustrated by the GFP⁺ OT-I T cell co-expression of KLRG1 and CX3CR1 that are characteristic of effector T cells (Fig 6E).

At 10 dpi, the splenic OT-I were a heterogeneous population based on KLRG1 and CX3CR1 (Fig 3A) but by 6 weeks post infection, when these cells did not express Nur77-GFP (Fig 2B) there was a more homogeneous (>98%) population of OT-I that maintained a KLRG1⁺CX3CR1⁺ phenotype (Fig 7A). In contrast, in the brain, the vast majority of OT-I were not positive for CX3CR1 and varied in KLRG1 expression (Fig 7A). In the CNS, segregation by UMAP of the OT-I from 2 and 6 weeks post infection were markedly different phenotypically (Fig 7B). At the 6 week timepoint, approximately 15% of OT-I in the brain were Nur77-GFP⁺ (Fig 4B). Brain OT-I formed 9 unique clusters (with Nur77-GFP excluded from the UMAP analysis), a subset of GFP⁺ OT-I clustered differently than GFP⁻ OT-I by UMAP (Fig 7C). As in the early phase of the T cell response in the brain, KLRG1, Bcl-2, CD25, and Ki67 expression were higher on GFP⁺ OT-I (Fig 7D and 7E) and recent TCR activation was still strongly predictive of IFN-γ expression (Fig 7F). These data demonstrate that TCR stimulation contributes to the heterogeneity seen in the CD8⁺ T cell population in the CNS during early and late stages of infection. However, there remains considerable diversity of the Nur77-GFP⁻ OT-I population, that is not explained by recent TCR stimulation.

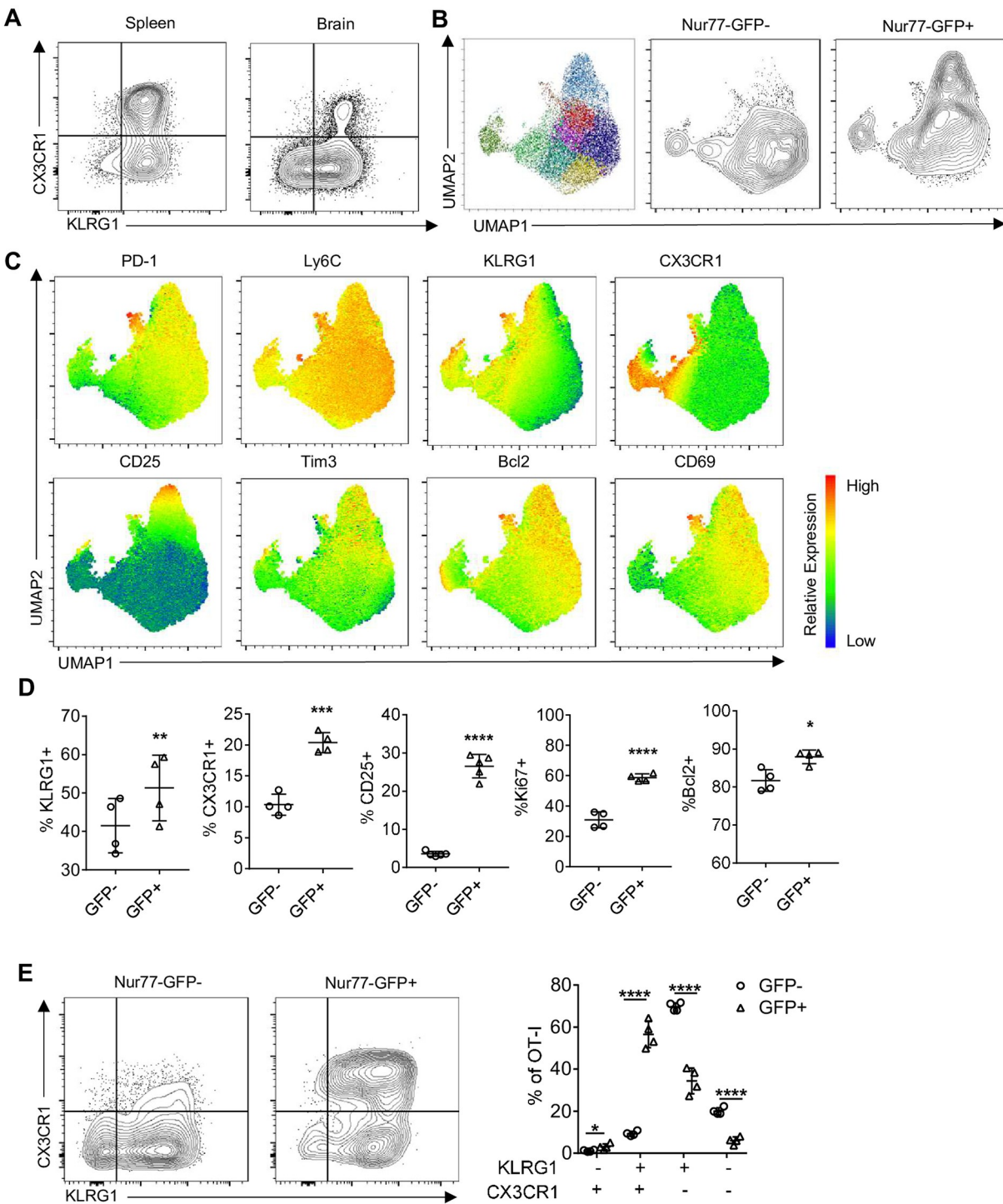


Fig 6. Infection induced phenotype of CNS *T. gondii* specific CD8⁺ T cells during early infection. (A) Phenotype of OT-I in spleen (left) and brain (right) of *T. gondii*-OVA infected mice 14 dpi (representative of N = 4 mice per tissue). (B-E) High dimensional flow cytometry with UMAP and Phenograph clustering was performed on brain OT-I at 14 dpi (N = 4 mice). (B) UMAP segregation of clusters of all OT-I (left), Nur77-GFP⁺ OT-I (center), and Nur77-GFP⁺ OT-I (right). (C) Heatmap of marker expression from UMAP. (D-E) Frequency of marker positive OT-I within Nur77-GFP⁻ or Nur77-GFP⁺ OT-I fraction. P values based on Paired T-test *p<0.05 **p<0.01 ***p<0.001 ****p<0.0001; error bars indicate SD.

<https://doi.org/10.1371/journal.ppat.1010296.g006>

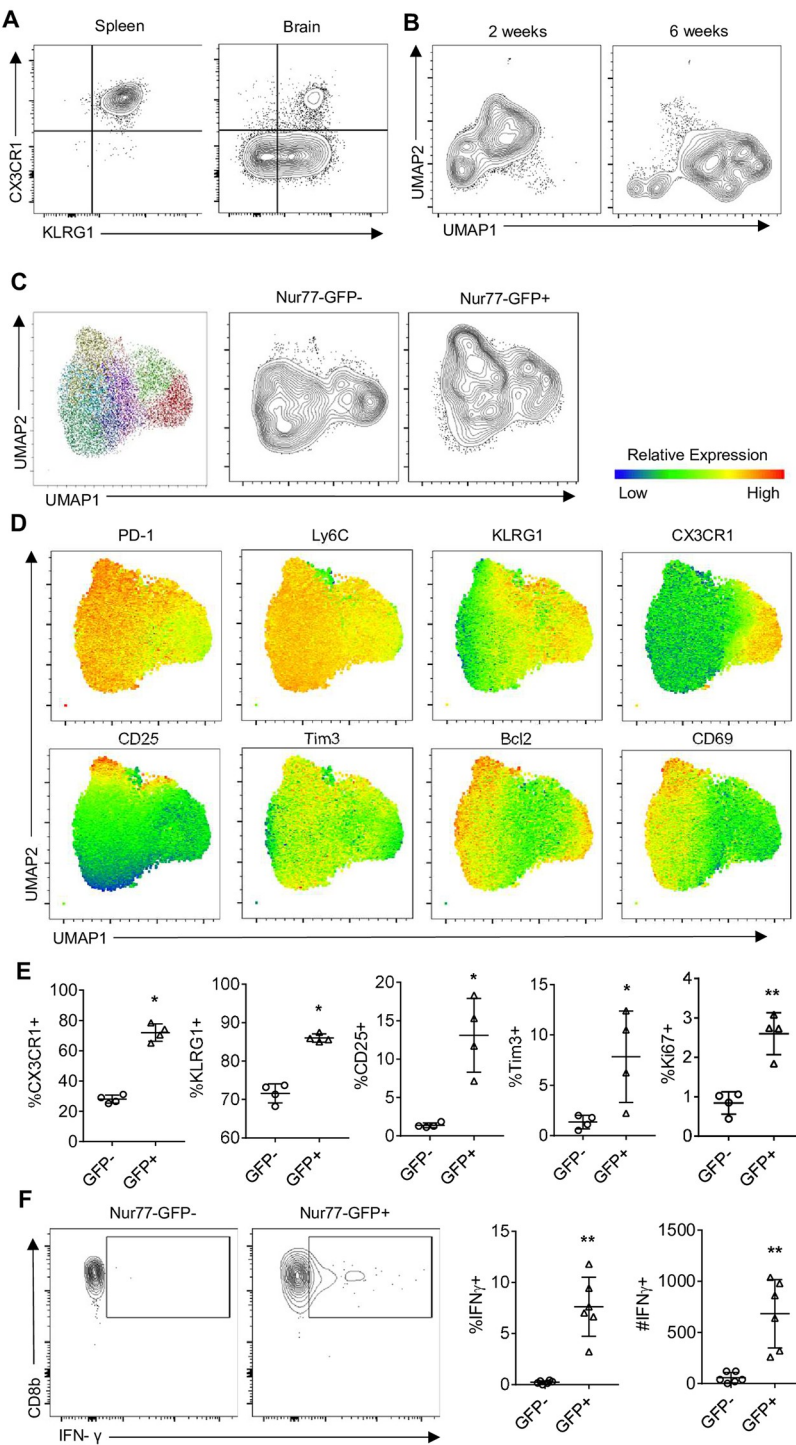


Fig 7. Infection induced phenotype and function of CNS *T. gondii* specific CD8⁺ T cells during chronic infection. (A) High dimensional flow cytometry with UMAP of OT-I from brains of mice infected with *T. gondii*-OVA at 14 dpi and 6 weeks post infection (representative of N = 4 mice per tissue). (B) Phenotype of OT-I in spleen and brain of *T. gondii*-OVA infected mice 6 weeks post infection (N = 4 mice per timepoint). (C-E) High dimensional flow cytometry with UMAP and Phenograph clustering was performed on brain OT-I at 6 weeks post infection (N = 4 mice). (C) UMAP segregation of clusters of all OT-I (left), Nur77-GFP⁺ OT-I (center), and Nur77-GFP⁺ OT-I (right). (D) Heatmap of marker expression from UMAP. I Frequency of marker positive OT-I within Nur77-GFP[−] or Nur77-GFP⁺ OT-I fraction. (F) Endogenous levels of IFN-γ expression in Nur77-GFP[−] and Nur77-GFP⁺ OT-I following 4-hour culture with protein transport inhibitor (N = 6 mice). P values based on Paired T-test *p<0.05 **p<0.01; error bars indicate SD.

<https://doi.org/10.1371/journal.ppat.1010296.g007>

Impact of parasite replication on TCR on TRM CD8⁺ T cell phenotype

The transcriptional profiling at day 14 indicated the presence of a Trm signature, consistent with the idea that continued local antigen stimulation may promote or maintain the formation of local Trm cells [70]. Indeed, at 6 weeks post infection, more than 50% of the GFP⁺ OT-I co-expressed CD69 and CD103 (Fig 8A). To address how antigen levels impact OT-I heterogeneity, *T. gondii*-OVA infected mice were treated with sulfadiazine, a drug that inhibits tachyzoite replication but does not have activity against bradyzoites [71], from days 21 to 49 post infection, and OT-I were subjected to high dimensional flow cytometry. As expected, based on the detection of tdTomato and PCR, treatment with sulfadiazine reduced parasite burden in the brain (Fig 8B). This was accompanied by a reduction in the percent of GFP⁺ OT-I, as well as the level of reporter expression per cell (Fig 8C). The OT-I isolated from the brains of sulfadiazine treated mice had partial differential clustering on UMAP (Fig 8D), and the most striking impact on this population was the loss of CX3CR1 expression by the GFP⁺ OT-I compared to vehicle treated mice (Fig 8E and 8F). Surprisingly, there was no significant change in the frequency or number of CD69⁺ CD103⁺ OT-I in the CNS (Fig 8E and 8G). These data sets establish that this population of Trm is not dependent on active parasite replication and suggest that antigen availability may influence Trm phenotype at an earlier stage of activation.

Discussion

Our previous studies have shown that during TE, parasite-specific CD8⁺ T cells are highly motile and based on their patterns of migration a mathematical model was developed for the ability of these cells to find infected targets [72]. In that report it was unclear what proportion or how frequently the parasite specific CD8⁺ T cells in the periphery or CNS re-encounter antigen and how this might influence effector function or fate. Here we show that TCR engagement in the periphery and the CNS correlates with levels of infection in these compartments and was as high as ~40% but fell to 10–15% in the chronic stage of infection in the CNS. Given that this Nur77 reporter only provides a snapshot of how many T cells have seen antigen within a narrow time frame it appears that the frequency with which CD8⁺ T cells encounter cognate antigen is high. Similarly, studies utilizing calcium flux reporters in the CNS of mice with high VSV titers concluded that up to 30% of pathogen specific CD8⁺ T cells were being stimulated by antigen over a short time period [25]. Thus, despite the CNS being a tissue canonically considered immune privileged during TE there are robust levels of antigen presentation [50–52] and secondary T cell activation that is required for local pathogen control.

While initial TCR stimulation is necessary for T cell priming, few studies have distinguished the role of subsequent antigen exposure on the function and fate of activated effector and memory CD8⁺ T cells *in vivo*. Many cytokines and transcription factors contribute to the development of T cell heterogeneity, and during toxoplasmosis these include the cytokines IL-7 and IL-12 [11,73], as well as transcription factors T-bet, c-Rel, BLIMP1, STAT1, and Blhhe40 [74–79], yet it is unclear whether secondary antigen encounter and TCR activation alters CD8⁺ T cell fate decisions. The studies presented here show that TCR engagement of activated CD8⁺ T cells in a secondary site of infection correlated with profound transcriptional changes and expression of markers of effector T cells (for example co-expression of KLRG1 and CX3CR1 and cytokine production). It has been proposed that TCR signal strength and levels of inflammation during priming influence the balance between effector and memory CD8⁺ T cells [66,80]. However, in the transfer studies performed here recent TCR signals did not appear to impact the ability to form a memory CD8⁺ T cell population. Likewise, the presence of Trm CD8⁺ T cells in the CNS have been described for other infections [81] and TCR signal strength and duration influences the establishment and function of these Trm populations.

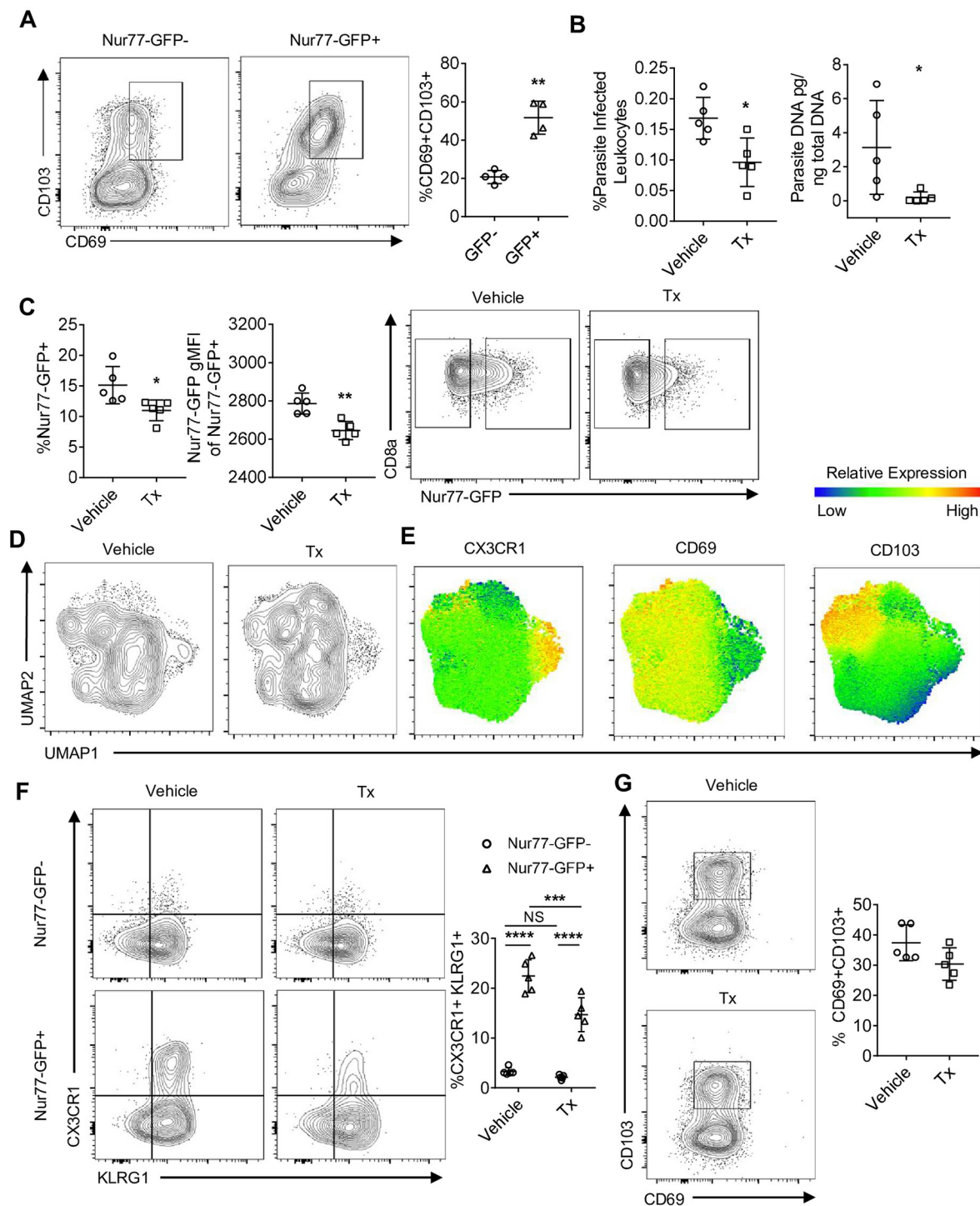


Fig 8. Impact of parasite replication of CNS CD8⁺ T cell phenotype. (A) Trm phenotype of OT-I at 6 weeks post infection in the brain (N = 4 mice). P values based on Paired T-test **p<0.01; error bars indicate SD. (B-G) *T. gondii*-OVA infected mice were treated with sulfadiazine from 3 weeks to 7 weeks post infection and parasite burden and OT-I phenotype was assessed at 7 weeks (N = 5 mice per group). (B) Frequency of parasite infected leukocytes per brain as measured by flow cytometry (left) and total brain parasite burden as measured by parasite PCR (right). P values based on Students T-test (B-C) or Two-Way ANOVA (F) *p<0.05 **p<0.01 ***p<0.001 ****p<0.0001; error bars indicate SD.

<https://doi.org/10.1371/journal.ppat.1010296.g008>

[82,83]. A Trm population has also been described during TE that produces IFN- γ and TNF- α [34] and the studies presented here revealed that the OT-I Trm-like cells received frequent TCR stimulation. However, while the absence of active parasite replication resulted in reduced TCR engagement there was no significant change in the frequency or number of these Trm cells in the CNS. Thus, both approaches that addressed the impact of secondary TCR activity on memory populations suggest that recent antigen encounter does not alter these fates and fit with the concept that Trm progenitors are generated early in effector responses [81,84]. Additionally, the use of sulfadiazine to restrict parasite replication, which may mimic chronic infection in humans, highlighted the persistence of the Trm population in the absence of replicating parasites. However, it is currently unclear whether parasite-specific Trm form in the CNS following *T. gondii* infection in humans, and whether these cells are critical in controlling chronic human disease.

The CNS represents a unique site of inflammation during infection, and the ability of *T. gondii* to establish a persistent infection in this tissue provides the opportunity to study how TCR signals intersect with different phases of the T cell response in the brain. For example, it has been suggested that following challenge with viral or bacterial infections that pathogen replication in the brain is not required for resident CD8 $^{+}$ T cell populations to populate the CNS [85]. However, during toxoplasmosis, endothelial cells of the blood brain barrier are infected [45] and the data that associates CX3CR1 (a chemokine receptor responsible for leukocyte entry into the CNS [86]) with TCR activation in the vascular compartment of the CNS implies that antigen stimulation at the blood brain barrier may induce T cell extravasation into the parenchyma. The use of the Nur77-GFP reporter as a surrogate for TCR activation should provide a sensitive system to assess the host factors that contribute to compartment (vascular, endothelial, and parenchymal) specific T cell activity in the CNS required for T cell mediated protective immunity.

In certain cancers and infection, one of the effects of repetitive antigen stimulation on CD8 $^{+}$ T cells is the induction of T cell exhaustion, denoted by an increase in inhibitory receptors and a decrease in cytokine secretion and cytolytic capacity [87–89]. During TE, parasite-specific T cells express high levels of inhibitory receptors such as PD-1 and TIGIT and it has been suggested that these T cell populations may be exhausted [88–91]. Indeed, there is a report that PD-L1 blockade leads to enhanced CD8 $^{+}$ T cell responses during TE [89], whereas in a similar setting the absence of TIGIT does not augment the T cell response [90]. The impact of inhibitory receptors during TE is complicated by evidence that PD-1 supports the generation of Trm in the CNS in viral infections [92–94]. Nonetheless, in our studies IFN- γ expression in the brain was closely correlated with expression of Nur77-GFP, indicating that TCR-independent bystander cytokine-mediated activation of CD8 $^{+}$ T cells [95–97] is not a major contributor to the production of IFN- γ . Moreover, the functional and transcriptional analysis did not reveal any early signs of exhaustion in Nur77-GFP $^{+}$ OT-I. Indeed, the magnitude of differentially expressed genes associated with TCR activation in the CNS was similar in scope to the transcriptional changes observed during priming of OT-I T cells in other models [1]. Many of these upregulated genes were transcription factors and regulators (*Irf8*, *Batf3*, *Bach2*, *Egr2*) known to direct CD8 $^{+}$ T cell function, indicating that subsequent antigen encounter may restructure transcriptional programs. These results also revealed six clusters that were not segregated by Nur77-GFP expression and underscore the need for additional studies to distinguish how priming affects diversity versus the TCR-independent signals that affect the evolution of the T cell response during TE.

There are several neurotropic infections that have distinct developmental states associated with latency and for *T. gondii* this is exemplified by the ability to form the tissue cyst. It has been proposed that the presence of this stage in neurons, a cell type known for low MHC-I

expression [98], would be sequestered by the immune response. There is good evidence that *T. gondii* antigen is readily presented to T cells within the CNS [50,51,99], and the idea that neurons can act as a refuge has been challenged by evidence that MHC-I presentation of tachyzoite antigens by neurons contributes to parasite control [52]. Imaging of brains from mice chronically infected with *T. gondii* had higher numbers of Nur77-GFP⁺ OT-I surrounding tachyzoites but as the infection in the brain progresses the decline in levels of TCR engagement correlated with parasite control and the switch from tachyzoite to bradyzoite. However, there were examples where Nur77-GFP⁺ OT-I were in close proximity to intact cysts but whether this is due to presentation by infected neurons, other glial populations, or infiltrating DC or monocyte populations that interact with infected neurons [51] is currently unknown. Whether the cyst stage is under direct immune surveillance is also unclear but the ability of bradyzoites to actively block IFN- γ signaling [48] implies the need for the parasite to evade an active response against the cyst stage [44,100]. Currently, there is a paucity of host and parasite specific tools to dissect the ability of host cells to process and present antigens from the bradyzoite life-stage. Future experiments utilizing bradyzoite-specific secretion of model antigens combined with the Nur77-GFP reporter will be utilized to address this knowledge gap.

Materials and methods

Ethics statement

All mice were housed in a specific-pathogen free environment at the University of Pennsylvania School of Veterinary Medicine in accordance with federal guidelines and with approval of the Institutional Animal Care and Use Committee.

Mice and infection

Nur77-GFP reporter mice, C57BL/6 mice, CD45.1 C57BL/6 mice, and OT-I mice were purchased from Jackson Laboratories (for all materials and reagents, see Tables 1 and 2). DPE-GFP transgenic mice were originally obtained from Ulrich H. von Andrian (CBR, Harvard, Boston MA) and were crossed to OT-I mice. Group sizes for experiments were between 3–6 mice and are indicated in figure legends. The generation of CPS-OVA parasites and PRU-OVA parasites were described previously [29,62].

Parasites were cultured and maintained by serial passage on human foreskin fibroblast cells in the presence of parasite culture media (DMEM, 20% medium M199, 10% fetal bovine serum (FBS), 1% penicillin-streptomycin, 25 μ g/ml gentamycin) which was supplemented with uracil for culturing CPS strain parasites (final concentration of 0.2 mM uracil). Tachyzoites of each strain were prepared for infection by serial 26g needle passage and filtered through a 5- μ m-pore-size filter. 1 day prior to infection, 5,000 congenically distinct naive splenic Nur77-GFP OT-I were transferred i.v. into naive mice. Mice were infected i.p. with 10^4 live parasites. In indicated experiments, mice were treated with 250mg/L of sulfadiazine in drinking water for 4 weeks beginning at 3 weeks post infection.

For adoptive transfers of OT-I from infected mice to naive mice, OT-I were double sorted on a BD FACS Aria. Each naive mice received an i.v. transfer of 150,000 Nur77-GFP⁻ or Nur77-GFP⁺ pooled from 2 infected mice. Recipient mice were treated with sulfadiazine two days prior and 1 week following transfer to ensure *T. gondii* infection was not transferred.

Parasite quantification by PCR

Approximately 10mg of tissue was snap frozen and DNA was extracted with Qiagen DNeasy Blood and Tissue Kit according to manufacturer's protocol. Real-time PCR was conducted

Table 1. Materials.

Fluorophore	Target	Clone	Catalog #	Source
BUV395	KLRG1	2F1	740279	Becton Dickinson (Franklin Lakes, NJ)
BUV563	CD8a	53–6.7	748535	Becton Dickinson
BUV615	Va2	B20.1	751416	Becton Dickinson
BUV661	IL2Rb	TM-β1	741493	Becton Dickinson
BUV737	CD69	H1.2F3	612793	Becton Dickinson
BUV805	CD11a	2D7	741919	Becton Dickinson
BV421	PD-1	29F.1A12	135218	BioLegend (San Diego, CA)
AQUA	Viability		13–0870	Tonbo Biosciences (San Diego, CA)
BV570	Ly6c	HK1.4	128030	BioLegend
BV605	CD103	2E7	121433	BioLegend
BV650	CD25	PC61	102038	BioLegend
BV711	CD45.1	A20	110739	BioLegend
BV785	CX3CR1	SA011F11	149029	BioLegend
APCef780	CD62L	MEL-14	47-0621-82	eBioscience (San Diego, CA)
PE	Tim3	134004	B8.2C12	BioLegend
PECy7	CD127	A7R34	135014	BioLegend
Unconjugated	BIM	K.912.7	MA5-14848	Invitrogen (Waltham, MA)
AF350	goat anti-rabbit	Polyclonal	A-11046	Invitrogen
AF488	GFP	FM264G	338008	BioLegend
BV480	Ki67	B56	566109	Becton Dickinson
AF647	Bcl2	BCL/10C4	633510	BioLegend
PECY5	Tbet	4B10	15-5825-82	eBioscience
AF700	CD45	30-F11	103128	BioLegend
PECy7	CD107a	1D4B	121620	BioLegend
AF647	CD45.1	A20	110720	BioLegend
APC	IFN-γ	XMG1.2	17-7311-82	Invitrogen
BV711	TNFα	MP6-XT22	506349	BioLegend
PECy7	CD8b	53–5.8	140416	BioLegend

<https://doi.org/10.1371/journal.ppat.1010296.t001>

with SYBR Green master mix according to manufacturer's protocol, with 500ng of template DNA. *T. gondii* DNA was amplified with forward (5'-TCCCCTCTGCTGGCGAAAGT-3') and reverse (5'-AGCGTTCTGTGGTCAACTATCGATTG-3') primers to the B1 gene. PCR was performed on an Applied Biosystems ViiA7 with the following cycle conditions: Hold phase: 2min 50C, 10min 95C; PCR phase (occurs 50x): 15s at 95C, 1min @60C.

Tissue processing

Spleens were grinded through a 70uM filter and red blood cells lysed with ACK lysis buffer. Brains were chopped into 1mm sections and incubated at 37C for 1.5 hours with 250ug/mL Collagenase/Dispase and 10ug/mL DNase, passed through a 70uM filter, then leukocytes were isolated through 30% and 60% Percoll density centrifugation.

Quantification of T cell cytokine production

1x10⁶ brain mononuclear cells were cultured *ex vivo* at 37C for 4 hours in RPMI supplemented with 10% FBS. For restimulations, 1uM of peptide was added with Protein Transport Inhibitor Cocktail. For quantification of endogenous levels of cytokine production, only Protein Transport Inhibitor Cocktail was added.

Table 2. Reagents.

Reagent	Source	Catalog #
C57Bl/6 Mice	Jackson Laboratories	000664
CD45.1 C57Bl/6 Mice	Jackson Laboratories	002014
Nur77-GFP Mice	Jackson Laboratories	016617
OT-I Mice	Jackson Laboratories	003831
DNeasy Blood and Tissue Kit	Qiagen	69506
ProLong Diamond Antifade Mountant with DAPI	Invitrogen	P36962
SIINFEKL peptide	Biosyn	Custom
SIIVFEKL peptide	Biosyn	Custom
SIIQFEKL peptide	Biosyn	Custom
EIINFEKL peptide	Biosyn	Custom
Protein Transport Inhibitor Cocktail	eBioscience	00-4980-93
DMEM Media	Corning	15017CV
M199 Media	Gibco	11150059
RPMI	Corning	10041CM
Fetal Bovine Serum	Sigma-Aldrich	F0926
Penicillin-Streptomycin	Gibco	15140122
Gentamycin	Gibco	15710064
Sulfadiazine	Sigma-Aldrich	S8626
SYBR Green Master Mix	Applied Biosystems	4309155
Collagenase/Dispase	Roche	10269638001
Dnase I	Roche	10104159001
Percoll	GE Healthcare	17-0891-01
CD8+ T Cell Isolation Kit, mouse	Miltenyi Biotec	130-104-075
Paraformaldehyde	ProSciTech	15710-S
Sucrose	Sigma-Aldrich	57-50-1
Triton-X100	ThermoFisher	28313
Tween-20	Sigma-Aldrich	P1379
Buffer RLT Plus	Qiagen	1053393
RNeasy Micro Plus Kit	Qiagen	74034
High Sensitivity RNA ScreenTape	Agilent	5067-5579
High Sensitivity RNA Ladder	Agilent	5067-5581
High Sensitivity RNA Buffer	Agilent	5067-5580
AMPure XP beads	Beckman Coulter	A63881
Foxp3 / Transcription Factor Staining Buffer Set	eBioscience	00-5523-00

<https://doi.org/10.1371/journal.ppat.1010296.t002>

Bone marrow macrophage culture

Bone marrow macrophages were isolated and cultured for 7 days with 30% L929 media in DMEM with 10% FBS, with media replenishing on day 4 after isolation. For peptide stimulations, 1uM of peptide was added to macrophages for 20 minutes and excess peptide was removed by washing 2 times. For parasite infection, a parasite to macrophage infection ratio of 2:1 was used, and excess parasites were removed by washing 2 times. CD8⁺ T cell were isolated by MACS bead enrichment. Macrophages and T cells were cultured at a 1:2 ratio.

Flow cytometry

Staining of extracellular antigens was performed following Fc receptor blocking with Rat IgG and anti-mouse CD16/CD32. Intracellular antigens were stained following fixation and

permeabilization using the FoXP3 Transcription Factor Staining Buffer Set. All samples were run on a BD FACSymphony A5 or BD FACSCanto and analyzed on FlowJo v10 software (FlowJo, Ashland, OR). UMAP and Phenograph were utilized in FlowJo for dimensionality reduction and unsupervised clustering.

Imaging

Brains were fixed in 4% paraformaldehyde overnight, followed by 15% and 30% sucrose in PBS overnight. 12uM sections were stained with AF488 anti-GFP and AF647 anti-CD45.1 in 0.1% Triton-X100 and 0.05% Tween-20 in PBS. Slides were sealed with Prolong Diamond Antifade Mountant with DAPI. Slides were imaged at 60x magnification on a Leica SP5-II (Leica, Wetzlar, Germany).

Live imaging of brain explants was performed as previously described [72]. Briefly, mice were infected with PRU-OVA parasites expressing tdTomato. Four weeks following infection, mice received 2×10^6 activated DPE-GFP-OT-I i.v., and brains were imaged one week following transfer of DPE-GFP-OT-I. Imaging was performed on a Leica SP5 multiphoton.

RNA sequencing

Nur77-GFP- and Nur77-GFP+ OT-I were double sorted as described above. Cells were collected in RPMI with 20% FBS and resuspended in Buffer RLT Plus. mRNA was isolated using RNeasy Micro Plus Kit and RNA quality was evaluated by High Sensitivity RNA Screen Tape on an Agilent 4200 TapeStation. cDNA library was prepared with Takara SMART-Seq HT kit and adapters ligated with Nextera XT DNA Library Preparation Kit and Index Kit v2 according to manufacturers' protocols. AMPure XP beads were used for primer cleanup. 75-base pair reads were sequenced on a NextSeq 500 machine (Illumina, San Diego, CA) according to manufacturer protocol. Kallisto was utilized to pseudo-align genes to version 75 of the mouse reference genome GRCm38. Transcripts that were represented in fewer than 3 of 4 samples in a group were excluded from analysis. The limma package in R was used to generate normalized counts per million, and differential genes (adjusted P-value > 0.05) were identified with a log fold change cutoff of 0.3. The heatmaply package was used for heatmap generation. Gene set enrichment analysis was performed with GSEA software (v4.0.3, Broad Institute) with gene sets containing less than 10 genes excluded. Enrichment plots were generated in Cytoscape (v3.7.1) with an adjusted P-value cutoff of 0.05 and false discovery rate cutoff of 0.1 (pipeline adapted from [101]). Data is deposited in GEO (accession# GSE188495).

Supporting information

S1 Movie. Ex vivo imaging of OT-I in the CNS of *T. gondii* infected mice. Behavior of constitutive GFP OT-I T cells (green) in the brains of mice infected with *T. gondii*-OVA (red). OT-I were transferred into chronically infected mice and imaged one week post transfer. Live imaging of brain explants.

(MOV)

S1 Fig. Effect of TCR signal strength on Nur77-GFP OT-I reporter activity. (A) Peptide pulsed splenocytes were incubated with Nur77-GFP OT-I and reporter activity was assessed at 3 hours (N = 2 technical replicates).

(TIF)

S2 Fig. Transfer of Nur77-GFP OT-I from *T. gondii* infected mice into naive mice. (A) FMO based gating for KLRL1 and CX3CR1 for Fig 3A. (B-E) OT-I from spleen of *T. gondii*-OVA 10 dpi were sorted by Nur77-GFP expression and transferred into naive mice. Mice were

sacrificed 14 days post transfer (N = 4 mice). Lack of infection at 14 days post transfer measured by (B) tdTomato expression of total splenocytes or (C) Nur77-GFP expression in transferred OT-I. (D) FMO based gating for KLRG1 and CX3CR1 for Fig 3E. (E) KLRG1 and CXCR3 expression of Nur77-GFP⁻ and Nur77-GFP⁺ OT-I prior to transfer at 10 dpi and 14 days post transfer. P values based on Two-Way ANOVA; error bars indicate SD. (TIF)

S3 Fig. Transcriptional profiling of Nur77-GFP OT-I from CNS. (A-B) Nur77-GFP⁻ and Nur77-GFP⁺ OT-I from the brains of mice infected with *T. gondii*-OVA 14 dpi were transcriptionally profiled using RNA-sequencing (N = 4 pools of 2 mice per pool). (A) PCA plot of Nur77-GFP⁻ and Nur77-GFP⁺ OT-I. (B) Endogenous cytokine production of Nur77-GFP⁻ and Nur77-GFP⁺ OT-I from the CNS of *T. gondii*-OVA infected mice at 14 dpi. (TIF)

S1 Data. Excel spreadsheet containing numerical values for all graphs in primary and supplemental figures.

(XLSX)

S1 Table. GSEA enrichment of Nur77-GFP OT-I from the CNS of *T. gondii* infected mice. Nur77-GFP⁻ and Nur77-GFP⁺ OT-I from the brains of mice infected with *T. gondii*-OVA 14 dpi were transcriptionally profiled using RNA-sequencing (N = 4 pools of 2 mice per pool). Top GSEA gene sets with FDR>0.05 enriched in Nur77-GFP⁺ OT-I compared to Nur77-GFP⁻ OT-I. (TIF)

Author Contributions

Conceptualization: Lindsey A. Shallberg, Christopher A. Hunter.

Data curation: Lindsey A. Shallberg.

Formal analysis: Lindsey A. Shallberg.

Funding acquisition: Anita A. Koshy, Christopher A. Hunter.

Investigation: Lindsey A. Shallberg, Anthony T. Phan, Breanne E. Haskins, Tajie H. Harris.

Methodology: Joseph A. Perry.

Resources: Anita A. Koshy.

Software: Daniel P. Beiting.

Supervision: Anthony T. Phan, David A. Christian, Daniel P. Beiting, Christopher A. Hunter.

Writing – original draft: Lindsey A. Shallberg, Christopher A. Hunter.

Writing – review & editing: Lindsey A. Shallberg, David A. Christian, Daniel P. Beiting, Anita A. Koshy, Christopher A. Hunter.

References

1. Best JA, Blair DA, Knell J, Yang E, Mayya V, Doedens A, et al. Transcriptional insights into the CD8(+) T cell response to infection and memory T cell formation. *Nat Immunol*. 2013; 14(4):404–12. Epub 2013/02/12. <https://doi.org/10.1038/ni.2536> PMID: 23396170.
2. Wakim LM, Woodward-Davis A, Bevan MJ. Memory T cells persisting within the brain after local infection show functional adaptations to their tissue of residence. *Proc Natl Acad Sci U S A*. 2010; 107(42):17872–9. Epub 2010/10/07. <https://doi.org/10.1073/pnas.1010201107> PMID: 20923878.

3. Wakim LM, Woodward-Davis A, Liu R, Hu Y, Villadangos J, Smyth G, et al. The molecular signature of tissue resident memory CD8 T cells isolated from the brain. *J Immunol.* 2012; 189(7):3462–71. Epub 2012/08/28. <https://doi.org/10.4049/jimmunol.1201305> PMID: 22922816.
4. Henrickson SE, Perro M, Loughhead SM, Senman B, Stutte S, Quigley M, et al. Antigen availability determines CD8(+) T cell-dendritic cell interaction kinetics and memory fate decisions. *Immunity.* 2013; 39(3):496–507. Epub 2013/09/24. <https://doi.org/10.1016/j.jimmuni.2013.08.034> PMID: 24054328.
5. Butz EA, B M. Massive Expansion of Antigen-Specific CD8+ T Cells during an Acute Virus Infection. *Immunity.* 1998; 8(2):167–75. [https://doi.org/10.1016/s1074-7613\(00\)80469-0](https://doi.org/10.1016/s1074-7613(00)80469-0) PMID: 9491998.
6. Jameson SC, Masopust D. Understanding Subset Diversity in T Cell Memory. *Immunity.* 2018; 48(2):214–26. Epub 2018/02/22. <https://doi.org/10.1016/j.jimmuni.2018.02.010> PMID: 29466754.
7. Bottcher JP, Beyer M, Meissner F, Abdulla Z, Sander J, Hochst B, et al. Functional classification of memory CD8(+) T cells by CX3CR1 expression. *Nat Commun.* 2015; 6:8306. Epub 2015/09/26. <https://doi.org/10.1038/ncomms9306> PMID: 26404698.
8. Gerlach C, Moseman EA, Loughhead SM, Alvarez D, Zwijnenburg AJ, Waanders L, et al. The Chemo-Kine Receptor CX3CR1 Defines Three Antigen-Experienced CD8 T Cell Subsets with Distinct Roles in Immune Surveillance and Homeostasis. *Immunity.* 2016; 45(6):1270–84. Epub 2016/12/13. <https://doi.org/10.1016/j.jimmuni.2016.10.018> PMID: 27939671.
9. Herndler-Brandstetter D, Ishigame H, Shinnakasu R, Plajer V, Stecher C, Zhao J, et al. KLRG1(+) Effector CD8(+) T Cells Lose KLRG1, Differentiate into All Memory T Cell Lineages, and Convey Enhanced Protective Immunity. *Immunity.* 2018; 48(4):716–29 e8. Epub 2018/04/08. <https://doi.org/10.1016/j.jimmuni.2018.03.015> PMID: 29625895.
10. Badovinac VP, Haring JS, Harty JT. Initial T cell receptor transgenic cell precursor frequency dictates critical aspects of the CD8(+) T cell response to infection. *Immunity.* 2007; 26(6):827–41. Epub 2007/06/09. <https://doi.org/10.1016/j.jimmuni.2007.04.013> PMID: 17555991.
11. Kaech SM, Tan JT, Wherry EJ, Konieczny BT, Surh CD, Ahmed R. Selective expression of the interleukin 7 receptor identifies effector CD8 T cells that give rise to long-lived memory cells. *Nat Immunol.* 2003; 4(12):1191–8. Epub 2003/11/20. <https://doi.org/10.1038/ni1009> PMID: 14625547.
12. Chu HH, Chan SW, Gosling JP, Blanchard N, Tsitsiklis A, Lythe G, et al. Continuous Effector CD8(+) T Cell Production in a Controlled Persistent Infection Is Sustained by a Proliferative Intermediate Population. *Immunity.* 2016; 45(1):159–71. Epub 2016/07/17. <https://doi.org/10.1016/j.jimmuni.2016.06.013> PMID: 27421704.
13. Badovinac VP, Porter BB, Harty JT. Programmed contraction of CD8(+) T cells after infection. *Nat Immunol.* 2002; 3(7):619–26. Epub 2002/06/11. <https://doi.org/10.1038/ni804> PMID: 12055624.
14. Bachmann MF, Wolint P, Schwarz K, Jager P, Oxenius A. Functional properties and lineage relationship of CD8+ T cell subsets identified by expression of IL-7 receptor alpha and CD62L. *J Immunol.* 2005; 175(7):4686–96. Epub 2005/09/24. <https://doi.org/10.4049/jimmunol.175.7.4686> PMID: 16177116.
15. Jin X, B D, Tuttleton SE, Lewin S, Gettie A, Blanchard J, Irwin CE, Safrit JT, Mittler J, Weinberger L, Kostrakis LG, Zhang L, Perelson AS, Ho DD. Dramatic rise in plasma viremia after CD8(+) T cell depletion in simian immunodeficiency virus-infected macaques. *J Exp Med.* 189(6):991–8. <https://doi.org/10.1084/jem.189.6.991> PMID: 10075982.
16. Suzuki Y, R J. Dual regulation of resistance against *Toxoplasma gondii* infection by Lyt-2+ and Lyt-1+, L3T4+ T cells in mice. *J Immunol.* 1988; 140(11):3943–6. PMID: 3259601.
17. Fröhlich A, Kisielow J, Schmitz I, Freigang S, Shamshiev AT, Weber J, et al. IL-21R on T Cells Is Critical for Sustained Functionality and Control of Chronic Viral Infection. *Science.* 2009; 324(5934):1576–80. <https://doi.org/10.1126/science.1172815> PMID: 19478140.
18. Paley MA, Kroy DC, Odorizzi PM, Johnnidis JB, Dolfi DV, Barnett BE, et al. Progenitor and Terminal Subsets of CD8+ T Cells Cooperate to Contain Chronic Viral Infection. *Science.* 2012; 338(6111):1220–5. <https://doi.org/10.1126/science.1229620> PMID: 23197535.
19. Gerlach C, R J, Perié L, van Rooij N, van Heijst JW, Velds A, Urbanus J, Naik SH, Jacobs H, Beltman JB, de Boer RJ, Schumacher TN. Heterogeneous differentiation patterns of individual CD8+ T cells. *Science.* 2014; 340:635–9. <https://doi.org/10.1126/science.1235487> PMID: 23493421.
20. Suresh M, Whitmire JK, Harrington LE, Larsen CP, Pearson TC, Altman JD, et al. Role of CD28-B7 interactions in generation and maintenance of CD8 T cell memory. *J Immunol.* 2001; 167(10):5565–73. Epub 2001/11/08. <https://doi.org/10.4049/jimmunol.167.10.5565> PMID: 11698427.
21. Byers AM, Kemball CC, Moser JM, Lukacher AE. Cutting edge: rapid in vivo CTL activity by polyoma virus-specific effector and memory CD8+ T cells. *J Immunol.* 2003; 171(1):17–21. Epub 2003/06/21. <https://doi.org/10.4049/jimmunol.171.1.17> PMID: 12816977.

22. Murphy EE, T G, Macatonia SE, Hsieh CS, Mattson J, Lanier L, Wysocka M, Trinchieri G, Murphy K, O'Garra A. B7 and interleukin 12 cooperate for proliferation and interferon gamma production by mouse T helper clones that are unresponsive to B7 costimulation. *J Exp Med.* 1994; 180(1):223–31. <https://doi.org/10.1084/jem.180.1.223> PMID: 7516409
23. Lertmemongkolchai G, Cai G, Hunter CA, Bancroft GJ. Bystander activation of CD8+ T cells contributes to the rapid production of IFN-gamma in response to bacterial pathogens. *J Immunol.* 2001; 166(2):1097–105. Epub 2001/01/06. <https://doi.org/10.4049/jimmunol.166.2.1097> PMID: 11145690.
24. Yang J MT, Ouyang W, Murphy KM. Induction of interferon-gamma production in Th1 CD4+ T cells: evidence for two distinct pathways for promoter activation. *Eur J Immunol.* 1999; 29(2):548–55. [https://doi.org/10.1002/\(SICI\)1521-4141\(199902\)29:02<548::AID-IMMU548>3.0.CO;2-Z](https://doi.org/10.1002/(SICI)1521-4141(199902)29:02<548::AID-IMMU548>3.0.CO;2-Z) PMID: 10064070
25. Moseman EA, B A, Nayak D, McGavern DB. T cell engagement of cross-presenting microglia protects the brain from a nasal virus infection. *Science Immunology.* 2020; 8(48). <https://doi.org/10.1126/sciimmunol.abb1817> PMID: 32503876
26. Baaten BJ, Tinoco R, Chen AT, Bradley LM. Regulation of Antigen-Experienced T Cells: Lessons from the Quintessential Memory Marker CD44. *Front Immunol.* 2012; 3:23. Epub 2012/05/09. <https://doi.org/10.3389/fimmu.2012.00023> PMID: 22566907.
27. Reinhardt RL, Liang HE, Locksley RM. Cytokine-secreting follicular T cells shape the antibody repertoire. *Nat Immunol.* 2009; 10(4):385–93. Epub 2009/03/03. <https://doi.org/10.1038/ni.1715> PMID: 19252490.
28. Kiner E, Willie E, Vijaykumar B, Chowdhary K, Schmutz H, Chandler J, et al. Gut CD4(+) T cell phenotypes are a continuum molded by microbes, not by TH archetypes. *Nat Immunol.* 2021; 22(2):216–28. Epub 2021/01/20. <https://doi.org/10.1038/s41590-020-00836-7> PMID: 33462454.
29. Jordan KA, Wilson EH, Tait ED, Fox BA, Roos DS, Bzik DJ, et al. Kinetics and phenotype of vaccine-induced CD8+ T-cell responses to *Toxoplasma gondii*. *Infect Immun.* 2009; 77(9):3894–901. Epub 2009/06/17. <https://doi.org/10.1128/IAI.00024-09> PMID: 19528214.
30. Shah S, Grotenbreg GM, Rivera A, Yap GS. An extrafollicular pathway for the generation of effector CD8(+) T cells driven by the proinflammatory cytokine, IL-12. *Elife.* 2015;4. Epub 2015/08/06. <https://doi.org/10.7554/elife.09017> PMID: 26244629.
31. Warnock RA, A S, Butcher EC, von Andrian UH. Molecular mechanisms of lymphocyte homing to peripheral lymph nodes. *J Exp Med.* 1998; 187(2):205–16. <https://doi.org/10.1084/jem.187.2.205> PMID: 9432978
32. Masopust D, Vezys V, Usherwood EJ, Cauley LS, Olson S, Marzo AL, et al. Activated primary and memory CD8 T cells migrate to nonlymphoid tissues regardless of site of activation or tissue of origin. *J Immunol.* 2004; 172(8):4875–82. Epub 2004/04/07. <https://doi.org/10.4049/jimmunol.172.8.4875> PMID: 15067066.
33. Ariotti S, Haanen JB, Schumacher TN. Behavior and function of tissue-resident memory T cells. *Adv Immunol.* 2012; 114:203–16. Epub 2012/03/28. <https://doi.org/10.1016/B978-0-12-396548-6.00008-1> PMID: 22449783.
34. Landrith TA, Sureshchandra S, Rivera A, Jang JC, Rais M, Nair MG, et al. CD103(+) CD8 T Cells in the *Toxoplasma*-Infected Brain Exhibit a Tissue-Resident Memory Transcriptional Profile. *Front Immunol.* 2017; 8:335. Epub 2017/04/21. <https://doi.org/10.3389/fimmu.2017.00335> PMID: 28424687.
35. Mackay LK, Rahimpour A, Ma JZ, Collins N, Stock AT, Hafon ML, et al. The developmental pathway for CD103(+)CD8+ tissue-resident memory T cells of skin. *Nat Immunol.* 2013; 14(12):1294–301. Epub 2013/10/29. <https://doi.org/10.1038/ni.2744> PMID: 24162776.
36. Moran AE, Holzapfel KL, Xing Y, Cunningham NR, Maltzman JS, Punt J, et al. T cell receptor signal strength in Treg and iNKT cell development demonstrated by a novel fluorescent reporter mouse. *J Exp Med.* 2011; 208(6):1279–89. Epub 2011/05/25. <https://doi.org/10.1084/jem.20110308> PMID: 21606508.
37. Low JS, Farsakoglu Y, Amezcu Vesely MC, Sefik E, Kelly JB, Harman CCD, et al. Tissue-resident memory T cell reactivation by diverse antigen-presenting cells imparts distinct functional responses. *J Exp Med.* 2020; 217(8). Epub 2020/06/12. <https://doi.org/10.1084/jem.20192291> PMID: 32525985 personal fees from the JEM Editorial Board outside the submitted work. No other disclosures were reported.
38. Ashouri JF, Weiss A. Endogenous Nur77 Is a Specific Indicator of Antigen Receptor Signaling in Human T and B Cells. *J Immunol.* 2017; 198(2):657–68. Epub 2016/12/13. <https://doi.org/10.4049/jimmunol.1601301> PMID: 27940659.
39. Zemmour D, Zilionis R, Kiner E, Klein AM, Mathis D, Benoist C. Single-cell gene expression reveals a landscape of regulatory T cell phenotypes shaped by the TCR. *Nat Immunol.* 2018; 19(3):291–301. Epub 2018/02/13. <https://doi.org/10.1038/s41590-018-0051-0> PMID: 29434354.

40. Headley MB, Bins A, Nip A, Roberts EW, Looney MR, Gerard A, et al. Visualization of immediate immune responses to pioneer metastatic cells in the lung. *Nature*. 2016; 531(7595):513–7. Epub 2016/03/17. <https://doi.org/10.1038/nature16985> PMID: 26982733.
41. Montoya JG, Liesenfeld O. Toxoplasmosis. *The Lancet*. 2004; 363(9425):1965–76. [https://doi.org/10.1016/s0140-6736\(04\)16412-x](https://doi.org/10.1016/s0140-6736(04)16412-x)
42. Parker SJ, R C, Alexander J. CD8+ T cells are the major lymphocyte subpopulation involved in the protective immune response to *Toxoplasma gondii* in mice. *Clin Exp Immunol*. 1991; 84(2):207–12. <https://doi.org/10.1111/j.1365-2249.1991.tb08150.x> PMID: 1902762
43. Hunter CA, Sibley LD. Modulation of innate immunity by *Toxoplasma gondii* virulence effectors. *Nat Rev Microbiol*. 2012; 10(11):766–78. Epub 2012/10/17. <https://doi.org/10.1038/nrmicro2858> PMID: 23070557.
44. Frickel EM, Hunter CA. Lessons from *Toxoplasma*: Host responses that mediate parasite control and the microbial effectors that subvert them. *J Exp Med*. 2021; 218(11). Epub 2021/10/21. <https://doi.org/10.1084/jem.20201314> PMID: 34670268.
45. Konradt C, Ueno N, Christian DA, Delong JH, Pritchard GH, Herz J, et al. Endothelial cells are a replicative niche for entry of *Toxoplasma gondii* to the central nervous system. *Nat Microbiol*. 2016; 1:16001. Epub 2016/08/31. <https://doi.org/10.1038/nmicrobiol.2016.1> PMID: 27572166.
46. Lambert H, Barragan A. Modelling parasite dissemination: host cell subversion and immune evasion by *Toxoplasma gondii*. *Cell Microbiol*. 2010; 12(3):292–300. Epub 2009/12/10. <https://doi.org/10.1111/j.1462-5822.2009.01417.x> PMID: 19995386.
47. Courret N, Darche S, Sonigo P, Milon G, Buzoni-Gatel D, Tardieu I. CD11c- and CD11b-expressing mouse leukocytes transport single *Toxoplasma gondii* tachyzoites to the brain. *Blood*. 2006; 107(1):309–16. Epub 2005/07/30. <https://doi.org/10.1182/blood-2005-02-0666> PMID: 16051744.
48. Rosenberg A, Sibley LD. *Toxoplasma gondii* secreted effectors co-opt host repressor complexes to inhibit necroptosis. *Cell Host Microbe*. 2021; 29. Epub 2021/05/28. <https://doi.org/10.1016/j.chom.2021.04.016> PMID: 34043960.
49. Hunter CA, Remington JS. Immunopathogenesis of toxoplasmic encephalitis. *J Infect Dis*. 1994; 170(5):1057–67. Epub 1994/11/01. <https://doi.org/10.1093/infdis/170.5.1057> PMID: 7963693.
50. Schaeffer M, Han S-J, Chtanova T, van Dooren GG, Herzmark P, Chen Y, et al. Dynamic Imaging of T Cell-Parasite Interactions in the Brains of Mice Chronically Infected with *Toxoplasma gondii*. *The Journal of Immunology*. 2009; 182(10):6379–93. <https://doi.org/10.4049/jimmunol.0804307> PMID: 19414791.
51. John B, Harris TH, Tait ED, Wilson EH, Gregg B, Ng LG, et al. Dynamic Imaging of CD8+ T Cells and Dendritic Cells during Infection with *Toxoplasma gondii*. *PLOS Pathogens*. 2009; 5(7):e1000505. <https://doi.org/10.1371/journal.ppat.1000505> PMID: 19578440.
52. Salvioni A, Belloy M, Lebourg A, Bassot E, Cantaloube-Ferrieu V, Vasseur V, et al. Robust Control of a Brain-Persisting Parasite through MHC I Presentation by Infected Neurons. *Cell Rep*. 2019; 27(11):3254–68 e8. Epub 2019/06/13. <https://doi.org/10.1016/j.celrep.2019.05.051> PMID: 31189109.
53. Casciotti L, Ely KH, Williams ME, Khan IA. CD8(+)T-cell immunity against *Toxoplasma gondii* can be induced but not maintained in mice lacking conventional CD4(+) T cells. *Infect Immun*. 2002; 70(2):434–43. Epub 2002/01/18. <https://doi.org/10.1128/IAI.70.2.434-443.2002> PMID: 11796568.
54. Suzuki Y RJ. The effect of anti-IFN-gamma antibody on the protective effect of Lyt-2+ immune T cells against toxoplasmosis in mice. *J Immunol*. 1990; 144(5):1954–6. PMID: 2106557.
55. Yap GS, S A. Effector cells of both nonhemopoietic and hemopoietic origin are required for interferon (IFN)-gamma- and tumor necrosis factor (TNF)-alpha-dependent host resistance to the intracellular pathogen, *Toxoplasma gondii*. *J Exp Med*. 1999; 189(7):1083–92. <https://doi.org/10.1084/jem.189.7.1083> PMID: 10190899.
56. Wang ZD, Liu HH, Ma ZX, Ma HY, Li ZY, Yang ZB, et al. *Toxoplasma gondii* Infection in Immunocompromised Patients: A Systematic Review and Meta-Analysis. *Front Microbiol*. 2017; 8:389. Epub 2017/03/25. <https://doi.org/10.3389/fmicb.2017.00389> PMID: 28337191.
57. Wilson DC, Matthews S, Yap GS. IL-12 signaling drives CD8+ T cell IFN-gamma production and differentiation of KLRG1+ effector subpopulations during *Toxoplasma gondii* Infection. *J Immunol*. 2008; 180(9):5935–45. Epub 2008/04/22. <https://doi.org/10.4049/jimmunol.180.9.5935> PMID: 18424713.
58. Stumhofer JS, Silver JS, Hunter CA. IL-21 is required for optimal antibody production and T cell responses during chronic *Toxoplasma gondii* infection. *PLoS One*. 2013; 8(5):e62889. Epub 2013/05/15. <https://doi.org/10.1371/journal.pone.0062889> PMID: 23667536.
59. Khan IA, Moretto M, Wei XQ, Williams M, Schwartzman JD, Liew FY. Treatment with soluble interleukin-15Ralpha exacerbates intracellular parasitic infection by blocking the development of memory

- CD8+ T cell response. *J Exp Med.* 2002; 195(11):1463–70. Epub 2002/06/05. <https://doi.org/10.1084/jem.20011915> PMID: 12045244.
60. Collins MH, Craft JM, Bustamante JM, Tarleton RL. Oral exposure to *Trypanosoma cruzi* elicits a systemic CD8(+) T cell response and protection against heterotopic challenge. *Infect Immun.* 2011; 79(8):3397–406. Epub 2011/06/02. <https://doi.org/10.1128/IAI.01080-10> PMID: 21628516.
61. Dupont CD, Christian DA, Selleck EM, Pepper M, Leney-Greene M, Harms Pritchard G, et al. Parasite fate and involvement of infected cells in the induction of CD4+ and CD8+ T cell responses to *Toxoplasma gondii*. *PLoS Pathog.* 2014; 10(4):e1004047. Epub 2014/04/12. <https://doi.org/10.1371/journal.ppat.1004047> PMID: 24722202.
62. Pepper M, Dzierszinski F, Crawford A, Hunter CA, Roos D. Development of a system to study CD4+-T-cell responses to transgenic ovalbumin-expressing *Toxoplasma gondii* during toxoplasmosis. *Infect Immun.* 2004; 72(12):7240–6. Epub 2004/11/24. <https://doi.org/10.1128/IAI.72.12.7240-7246.2004> PMID: 15557649.
63. Gregg B, Dzierszinski F, Tait E, Jordan KA, Hunter CA, Roos DS. Subcellular antigen location influences T-cell activation during acute infection with *Toxoplasma gondii*. *PLoS One.* 2011; 6(7):e22936. Epub 2011/08/11. <https://doi.org/10.1371/journal.pone.0022936> PMID: 21829561.
64. Wilson EH, Harris TH, Mrass P, John B, Tait ED, Wu GF, et al. Behavior of parasite-specific effector CD8+ T cells in the brain and visualization of a kinesis-associated system of reticular fibers. *Immunity.* 2009; 30(2):300–11. Epub 2009/01/27. <https://doi.org/10.1016/j.immuni.2008.12.013> PMID: 19167248.
65. Christian DA, Adams TA, Smith TE, Shallberg LA, Theisen DJ, Phan AT, et al. cDC1 Coordinate Innate and Adaptive Responses in the Omentum required for T cell Priming and Memory. *bioRxiv.* 2020;2020.07.21.214809. <https://doi.org/10.1101/2020.07.21.214809>
66. Smith-Garvin JE, Burns JC, Gohil M, Zou T, Kim JS, Maltzman JS, et al. T-cell receptor signals direct the composition and function of the memory CD8+ T-cell pool. *Blood.* 2010; 116(25):5548–59. Epub 2010/09/18. <https://doi.org/10.1182/blood-2010-06-292748> PMID: 20847203.
67. Gazzinelli RT, Hieny S, Wynn TA, Wolf S, Sher A. Interleukin 12 is required for the T-lymphocyte-independent induction of interferon gamma by an intracellular parasite and induces resistance in T-cell-deficient hosts. *Proceedings of the National Academy of Sciences.* 1993; 90(13):6115–9. <https://doi.org/10.1073/pnas.90.13.6115> PMID: 8100999
68. Ferguson DJ, Graham DI, Hutchison WM. Pathological changes in the brains of mice infected with *Toxoplasma gondii*: a histological, immunocytochemical and ultrastructural study. *Int J Exp Pathol.* 1991; 72(4):463–74. Epub 1991/08/01. PMID: 1883744.
69. Watts E, Zhao Y, Dhara A, Eller B, Patwardhan A, Sinai AP. Novel Approaches Reveal that *Toxoplasma gondii* Bradyzoites within Tissue Cysts Are Dynamic and Replicating Entities In Vivo. *mBio.* 2015; 6(5):e01155–15. Epub 2015/09/10. <https://doi.org/10.1128/mBio.01155-15> PMID: 26350965.
70. Khan TN, Mooster JL, Kilgore AM, Osborn JF, Nolz JC. Local antigen in nonlymphoid tissue promotes resident memory CD8+ T cell formation during viral infection. *J Exp Med.* 2016; 213(6):951–66. Epub 2016/05/25. <https://doi.org/10.1084/jem.20151855> PMID: 27217536.
71. Ferreira RA, Oliveira AB, Ribeiro MF, Tafuri WL, Vitor RW. *Toxoplasma gondii*: in vitro and in vivo activities of the hydroxynaphthoquinone 2-hydroxy-3-(1'-propen-3-phenyl)-1,4-naphthoquinone alone or combined with sulfadiazine. *Exp Parasitol.* 2006; 113(2):125–9. Epub 2006/02/07. <https://doi.org/10.1016/j.exppara.2005.12.006> PMID: 16458300.
72. Harris TH, Banigan EJ, Christian DA, Konradt C, Tait Wojno ED, Norose K, et al. Generalized Levy walks and the role of chemokines in migration of effector CD8+ T cells. *Nature.* 2012; 486(7404):545–8. Epub 2012/06/23. <https://doi.org/10.1038/nature11098> PMID: 22722867.
73. Xiao Z, Casey KA, Jameson SC, Curtsinger JM, Mescher MF. Programming for CD8 T cell memory development requires IL-12 or type I IFN. *J Immunol.* 2009; 182(5):2786–94. Epub 2009/02/24. <https://doi.org/10.4049/jimmunol.0803484> PMID: 19234173.
74. Tsitsiklis A, Bangs DJ, Robey EA. CD8(+) T Cell Responses to *Toxoplasma gondii*: Lessons from a Successful Parasite. *Trends Parasitol.* 2019; 35(11):887–98. Epub 2019/10/12. <https://doi.org/10.1016/j.pt.2019.08.005> PMID: 31601477.
75. Harms Pritchard G, Hall AO, Christian DA, Wagage S, Fang Q, Muallem G, et al. Diverse roles for T-bet in the effector responses required for resistance to infection. *J Immunol.* 2015; 194(3):1131–40. Epub 2015/01/04. <https://doi.org/10.4049/jimmunol.1401617> PMID: 25556247.
76. Jordan KA, Dupont CD, Tait ED, Liou HC, Hunter CA. Role of the NF-κappaB transcription factor c-Rel in the generation of CD8+ T-cell responses to *Toxoplasma gondii*. *Int Immunol.* 2010; 22(11):851–61. Epub 2010/12/02. <https://doi.org/10.1093/intimm/dxq439> PMID: 21118906.

77. Hwang S, Cobb DA, Bhadra R, Youngblood B, Khan IA. Blimp-1-mediated CD4 T cell exhaustion causes CD8 T cell dysfunction during chronic toxoplasmosis. *J Exp Med.* 2016; 213(9):1799–818. Epub 2016/08/03. <https://doi.org/10.1084/jem.20151995> PMID: 27481131.
78. Lieberman LA, Banica M, Reiner SL, Hunter CA. STAT1 plays a critical role in the regulation of antimicrobial effector mechanisms, but not in the development of Th1-type responses during toxoplasmosis. *J Immunol.* 2004; 172(1):457–63. Epub 2003/12/23. <https://doi.org/10.4049/jimmunol.172.1.457> PMID: 14688355.
79. Yu F, Sharma S, Jankovic D, Gurram RK, Su P, Hu G, et al. The transcription factor Blhlhe40 is a switch of inflammatory versus antiinflammatory Th1 cell fate determination. *J Exp Med.* 2018; 215(7):1813–21. Epub 2018/05/19. <https://doi.org/10.1084/jem.20170155> PMID: 29773643.
80. Zehn D, Lee SY, Bevan MJ. Complete but curtailed T-cell response to very low-affinity antigen. *Nature.* 2009; 458(7235):211–4. Epub 2009/02/03. <https://doi.org/10.1038/nature07657> PMID: 19182777.
81. Netherby-Winslow CS, Ayers KN, Lukacher AE. Balancing Inflammation and Central Nervous System Homeostasis: T Cell Receptor Signaling in Antiviral Brain TRM Formation and Function. *Front Immunol.* 2020; 11:624144. Epub 2021/02/16. <https://doi.org/10.3389/fimmu.2020.624144> PMID: 33584727.
82. Frost EL, Lukacher AE. The importance of mouse models to define immunovirologic determinants of progressive multifocal leukoencephalopathy. *Front Immunol.* 2015; 5:646. Epub 2015/01/21. <https://doi.org/10.3389/fimmu.2014.00646> PMID: 25601860.
83. Maru S, Jin G, Schell TD, Lukacher AE. TCR stimulation strength is inversely associated with establishment of functional brain-resident memory CD8 T cells during persistent viral infection. *PLoS Pathog.* 2017; 13(4):e1006318. Epub 2017/04/15. <https://doi.org/10.1371/journal.ppat.1006318> PMID: 28410427.
84. Casey KA, Fraser KA, Schenkel JM, Moran A, Abt MC, Beura LK, et al. Antigen-independent differentiation and maintenance of effector-like resident memory T cells in tissues. *J Immunol.* 2012; 188(10):4866–75. Epub 2012/04/17. <https://doi.org/10.4049/jimmunol.1200402> PMID: 22504644.
85. Urban SL, Jensen IJ, Shan Q, Pewe LL, Xue H-H, Badovinac VP, et al. Peripherally induced brain tissue–resident memory CD8+ T cells mediate protection against CNS infection. *Nature Immunology.* 2020. <https://doi.org/10.1038/s41590-020-0711-8> PMID: 32572242.
86. Prinz M, Priller J. Tickets to the brain: role of CCR2 and CX3CR1 in myeloid cell entry in the CNS. *J Neuroimmunol.* 2010; 224(1–2):80–4. Epub 2010/06/18. <https://doi.org/10.1016/j.jneuroim.2010.05.015> PMID: 20554025.
87. Splitt SD SS, Valentine KM, Castellanos BE, Curd AB, Hoyer KK, Jensen KDC. PD-L1, TIM-3, and CTLA-4 Blockade Fails To Promote Resistance to Secondary Infection with Virulent Strains of Toxoplasma gondii. *Infection and Immunity.* 2018; 86(9). <https://doi.org/10.1128/IAI.00459-18> PMID: 29967089.
88. Bhadra R, Gigley JP, Khan IA. PD-1-mediated attrition of polyfunctional memory CD8+ T cells in chronic toxoplasma infection. *J Infect Dis.* 2012; 206(1):125–34. Epub 2012/04/28. <https://doi.org/10.1093/infdis/jis304> PMID: 22539813.
89. Bhadra R, Gigley JP, Weiss LM, Khan IA. Control of Toxoplasma reactivation by rescue of dysfunctional CD8+ T-cell response via PD-1-PDL-1 blockade. *Proc Natl Acad Sci U S A.* 2011; 108(22):9196–201. Epub 2011/05/18. <https://doi.org/10.1073/pnas.1015298108> PMID: 21576466.
90. Aldridge DL, Phan AT, de Waal Malefyt R, Hunter CA. Limited Impact of the Inhibitory Receptor TIGIT on NK and T Cell Responses during Toxoplasma gondii Infection. *Immunohorizons.* 2021; 5(6):384–94. Epub 2021/06/06. <https://doi.org/10.4049/immunohorizons.2100007> PMID: 34088852.
91. DeLong JH, O’Hara Hall A, Rausch M, Moodley D, Perry J, Park J, et al. IL-27 and TCR Stimulation Promote T Cell Expression of Multiple Inhibitory Receptors. *Immunohorizons.* 2019; 3(1):13–25. Epub 2019/07/30. <https://doi.org/10.4049/immunohorizons.1800083> PMID: 31356173.
92. Shwetank Frost EL, Mockus TE, Ren HM, Toprak M, Lauver MD, et al. PD-1 Dynamically Regulates Inflammation and Development of Brain-Resident Memory CD8 T Cells During Persistent Viral Encephalitis. *Front Immunol.* 2019; 10:783. Epub 2019/05/21. <https://doi.org/10.3389/fimmu.2019.00783> PMID: 31105690.
93. Shwetank, Abdelsame HA, Frost EL, Schmitz HM, Mockus TE, Youngblood BA, et al. Maintenance of PD-1 on brain-resident memory CD8 T cells is antigen independent. *Immunol Cell Biol.* 2017; 95(10):953–9. Epub 2017/08/23. <https://doi.org/10.1038/icb.2017.62> PMID: 28829048.
94. Prasad S, Hu S, Sheng WS, Chauhan P, Singh A, Lokengsard JR. The PD-1: PD-L1 pathway promotes development of brain-resident memory T cells following acute viral encephalitis. *J Neuroinflammation.* 2017; 14(1):82. Epub 2017/04/15. <https://doi.org/10.1186/s12974-017-0860-3> PMID: 28407741.

95. Berg RE, Crossley E, Murray S, Forman J. Memory CD8+ T cells provide innate immune protection against *Listeria monocytogenes* in the absence of cognate antigen. *J Exp Med.* 2003; 198(10):1583–93. Epub 2003/11/19. <https://doi.org/10.1084/jem.20031051> PMID: 14623912.
96. Soudja SM, Ruiz AL, Marie JC, Lauvau G. Inflammatory monocytes activate memory CD8(+) T and innate NK lymphocytes independent of cognate antigen during microbial pathogen invasion. *Immunity.* 2012; 37(3):549–62. Epub 2012/09/04. <https://doi.org/10.1016/j.immuni.2012.05.029> PMID: 22940097.
97. Chu T, Tyznik AJ, Roepke S, Berkley AM, Woodward-Davis A, Pattacini L, et al. Bystander-activated memory CD8 T cells control early pathogen load in an innate-like, NKG2D-dependent manner. *Cell Rep.* 2013; 3(3):701–8. Epub 2013/03/26. <https://doi.org/10.1016/j.celrep.2013.02.020> PMID: 23523350.
98. Lindå H HH, Cullheim S, Levinovitz A, Khademi M, Olsson T. Expression of MHC class I and beta2-microglobulin in rat spinal motoneurons: regulatory influences by IFN-gamma and axotomy. *Exp Neurol.* 1998; 150(2):282–95. <https://doi.org/10.1006/exnr.1997.6768> PMID: 9527898
99. Fischer HG, Bonifas U, Reichmann G. Phenotype and functions of brain dendritic cells emerging during chronic infection of mice with *Toxoplasma gondii*. *J Immunol.* 2000; 164(9):4826–34. Epub 2000/04/26. <https://doi.org/10.4049/jimmunol.164.9.4826> PMID: 10779791.
100. Shallberg LA, Hunter CA. Long live the king: *Toxoplasma gondii* nucleomodulin inhibits necroptotic cell death. *Cell Host Microbe.* 2021; 29(7):1165–6. Epub 2021/07/16. <https://doi.org/10.1016/j.chom.2021.06.010> PMID: 34265248.
101. Berry ASF, Farias Amorim C, Berry CL, Syrett CM, English ED, Beiting DP. An Open-Source Toolkit To Expand Bioinformatics Training in Infectious Diseases. *mBio.* 2021; 12(4):e0121421. Epub 2021/07/07. <https://doi.org/10.1128/mBio.01214-21> PMID: 34225494.